AD-A100 821 AIR FORCE INST OF TECH WRIGHT-PATTERSON AFB OH SCHOO--ETC F/G 17/8
OPTICAL PHASE ESTIMATION FROM INTEGRATED SAMPLES OF THE HETEROD--ETC(U)
DEC 80 M B MARK

UNCLASSIFIED AFIT/GEO/EE/80D-3

NL

1 OF 1
AD
A100821

END
DATE FILMED
7-81
DTIC

DDC

LEVEL II

AD A100821

DTIC FILE COPY

DTIC
ELECTE
JUL 1 1981
S D
D

DEPARTMENT OF THE AIR FORCE
AIR UNIVERSITY (ATC)

AIR FORCE INSTITUTE OF TECHNOLOGY

Wright-Patterson Air Force Base, Ohio

DISTRIBUTION STATEMENT A
Approved for public release;
Distribution Unlimited

81 6 30 042

Accession For
NTIS GRA&I
DTIC TAB
Unannounced
Justification
By
Distribution/
Availability Codes
Dist | Avail and/or Special
A

OPTICAL PHASE ESTIMATION FROM INTEGRATED SAMPLES OF THE HETERODYNED WAVEFRONT.

THESIS

AFIT/GEO/EE/80D-3

Martin B. Mark
2d Lt USAF

DTIC
ELECTE
JUL 1 1981
D

Approved for public release; distribution unlimited.

AFIT/GEO/EE/80D-3

OPTICAL PHASE ESTIMATION FROM INTEGRATED SAMPLES OF THE HETERODYNED WAVEFRONT

THESIS

Presented to the Faculty of the School of Engineering
of the Air Force Institute of Technology
in Partial Fulfillment of the
Requirements for the Degree of
Master of Science

by

Martin B. Mark, B.S.E.E.
Second Lieutenant, USAF
Graduate Electro-Optics
December 1980

Approved for public release; distribution unlimited.

Preface

The author wishes to thank Stanley R. Robinson, formerly of the AFIT Department of Electrical Engineering for proposing this topic. Also, the Optical Communications courses which he taught were of much help in tackling this problem. Thanks also go out to Prof. Peter Maybeck for answering several questions on Kalman filtering and also for publishing a readable book on the subject. Parts of his next book, not yet published, were also helpful and he deserves thanks for giving the author a copy of a chapter of the draft.

My thesis advisor, Prof. Ronald J. Carpinella, and the other committee members, Prof. James Moore and Prof. Donn Shankland, also deserve thanks in varying degrees. Prof. Carpinella was especially helpful in pointing the author in the right direction and pointing out tests or articles in journals which put this thesis on track. The author would finally like to thank Dr. Shankland for asking the subtle but important question, "What is phase?".

Martin B. Mark

Contents

		Page
Preface		ii
List of Figures		v
Abstract		vi
I.	Introduction	1
	Overview	3
II.	Receiver and Preprocessor Theoretical Background	4
	Optical Receiver Structure	4
	Preprocessor Structure	7
	Cramer-Rao Lower Bound	11
III.	Processor Determination: Maximum Likelihood Estimation	15
	Measurement Model Equations	15
	Maximum Likelihood Approach:Case(i)	16
	Maximum Likelihood Approach:Case(ii)	17
IV.	Processor Determination: State Variable Analysis and Kalman Filtering	19
	State and Variable Equations	19
	Processor Ambiguity	25
	Constant Phase	27
	Random Phase Walk	27
	Demodulation of FM Signals	30
	Phase Estimation with Frequency Uncertainty	34
V.	Simulation of Kalman Filter Processor	38
	Simulation Parameters	38
	Constant Phase Processor	40
	Random Phase Walk	44
	Phase Estimation with Doppler Shift	50
VI.	Conclusions and Recommendations	53
	Conclusions	53
	Recommendations	54

Bibliography 58
Appendix A 60
Appendix B 62
Appendix C 71
Vita 77

List of Figures

Figure		Page
1.	Receiver Schematic Diagram	5
2.	Maximum Likelihood Estimator	18
3a.	Constant Phase Processor Structure(Realization 1)	28
3b.	Constant Phase Processor Structure(Realization 2)	29
4a.	Random Walk Processor Structure (Realization 1)	31
4b.	Random Walk Processor Structure (Realization 2)	32
5.	Constant Phase Processor Output.	41
6.	Constant Phase Processor Bias.	43
7.	Constant Phase Processor Variance.	45
8.	Random Walk Processor Output Error	47
9.	Random Walk Processor Variances.	49

Abstract

A method for using integrating detectors to estimate the phase of an optical wavefront is investigated. The phase and amplitude are assumed to vary slowly compared to the integration time and the integrated samples are shown to be corrupted by white gaussian noise. A maximum a-posteriori nonlinear Kalman filter is derived and simulated for both constant and random walk phase processes. The performance of the filter is compared to its Cramer-Rao lower bound and a first order linearized phase-locked loop (PLL). The filter never performs a great deal better than the PLL, but it can be implemented in a low bandwidth system whereas the PLL assumes a wideband system.

The local oscillator is initially assumed to be stabilized in frequency and amplitude, and later a frequency shift is introduced. The filter manages to acquire and track the phase in a high carrier-to-noise ratio (CNR) environment although it does not estimate the frequency shift well. At 30 db CNR, the phase is estimated within about 0.02 radians, whereas the frequency shift estimation error is on the order of 500 kHz for a frequency shift of 2MHz.

OPTICAL PHASE ESTIMATION FROM INTEGRATED SAMPLES OF THE HETERODYNED WAVEFRONT

I. Introduction

The phase of an optical wavefront cannot be measured directly by a detector since this would require an extraordinarily fast detector and associated processing electronics. All presently used optical detectors respond only to the incident total optical power, not the instantaneous value of the E-field. Nevertheless, optical phase can be measured indirectly via several methods, most involving some sort of heterodyning system which moves the carrier coherently to a lower frequency where either the spatial or temporal characteristics of the resulting interference pattern can be examined (Ref.4:3301). Among other things, optical phase can be used to determine refractive index variations, examine transparent objects, perform nondestructive testing of surfaces, and reconstruction of an incident light wavefront (for instance, to correct aberrations in an actively compensated optical system, whether introduced by the optics or the atmosphere).

As is demonstrated in the theoretical development later in this paper, the output of a detector in an optical

receiver is at the heterodyne frequency, typically on the order of tens of megahertz or more. In order to pass this waveform, the detector must have a bandwidth of at least that much, and usually more if doppler shifts may be encountered. Such wideband detectors are expensive and not readily available in large array structures with uniform response characteristics. On the other hand, large uniform arrays of charge coupled devices (CCD's) are readily available. These devices do not have sufficient bandwidth to produce an output which is directly proportional to the heterodyned signal and thus produce a vector of outputs that are samples of the time integral of the heterodyned wavefront. That is, CCD's are photon counting detectors.

Interestingly, Wyant has shown (Ref.20:2624) that, in the absence of noise, it is possible to determine the phase of a wavefront from these integrated samples. The purpose of this paper is to extend and generalize Wyant's analysis and to analyze how well a system performs in the presence of corruption by white, gaussian noise.

In this paper, the phase of an optical field is defined as the argument of the received optical field phasor, $e^{j(2\pi f_0 t_0+\theta)}$ (in complex notation), minus the argument of the local oscillator phasor, $e^{j2\pi(f_0-f_{IF})t_0}$, minus $2\pi f_{IF}t_0$. The time t_0 is the time of the measurement, i.e., the time elapsed since the chosen origin time, $t=0$,

when phase was first defined. Clearly, without some sort of feedback between the received and local oscillator fields which defines a unique t=0 , (as is done in a PLL), the measured value of the phase will be a function of what t=0 is chosen. However, changes in the phase, whether temporal or spatial, will be invariant with respect to the choice of the origin of the time axis.

Overview

This paper begins with a general analysis of how the heterodyne or intermediate frequency (IF) signal comes about and a short description of why the white, gaussian noise (WGN) assumption is valid for the cases of interest. Next, the preprocessing forced on the system by the CCD detectors is examined and a Cramer-Rao lower bound for the error committed by any processor utilizing these samples to estimate phase is derived. Estimators are derived for various assumptions concerning the time correlation of the phase process using both maximum likelihood (ML) and state-variable approaches. Finally, the various processors are simulated and the results are presented and compared to the performance of a first order linearized phase-locked loop (PLL). This is a standard benchmark for comparisons in phase estimation problems. Throughout the paper, only one detector in the array is examined and no spatial information is incorporated.

II. Receiver and Preprocessor Theoretical Background

In this chapter, the optical heterodyne receiver is very briefly described and a justification for the WGN assumption is presented. Next, the preprocessor structure is examined and a Cramer-Rao (CR) lower bound is derived for any estimator using such processed samples. Some limiting assumptions are imposed on the bandwidths of the phase process and the amplitude variations of the IF signal. Finally, the Cramer-Rao bound is compared to that of a processor utilizing the signal without integration or sampling.

Optical Receiver Structure

An optical heterodyne reciever is shown schematically in Figure 1. The received field and the local oscillator field are both given in complex notation with an implied time dependence of $\exp(-j2\pi f_0 t)$, where f_0 is the mean optical frequency of the received field. Each element of the detector array responds to the total incident optical power. The output of the m,n-th detector is:

$$i_{mn}(t) = \frac{\eta}{hf_0} \int_{A_d} |U_R(x_m,y_n,t) + U_L(x_m,y_n,t) \exp[-j2\pi f_{IF} t]|^2 dx_m dy_n \qquad (1)$$

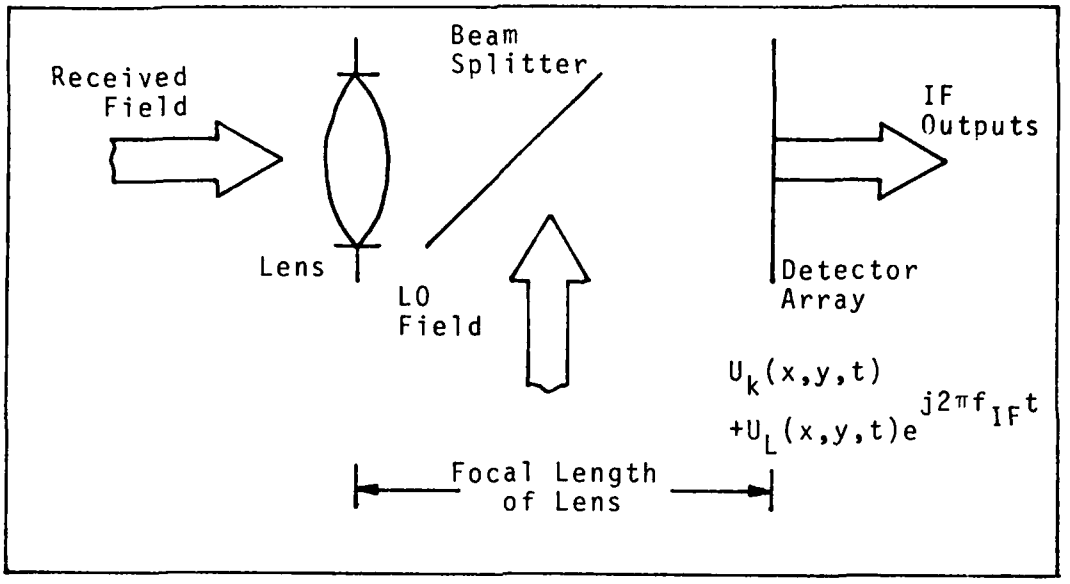

Figure 1. Receiver Schematic Diagram

$$= \frac{\eta}{hf_0} \int_{A_d} \left[|U_R(x_m,y_n,t)|^2 + |U_L(x_m,y_n,t)|^2 + 2\mathrm{Re}\{U_R(x_m,y_n,t) \cdot U_L^*(x_m,y_n,t)\exp\left[j2\pi f_{IF}t\right]\}\right] dx_m dy_n \quad (2)$$

$$= \frac{\eta}{hf_0} \int_{A_d} \{|U_R(x_m,y_n,t)|^2 + |U_L(x_m,y_n,t)|^2 + 2|U_R(x_m,y_n,t)| \cdot |U_L(x_m,y_n,t)| \cdot \cos(2\pi f_{IF}t + \theta(x_m,y_n,t))\} dx_m dy_n \quad (3)$$

Where η is the quantum efficiency of the detector, h is Planck's constant, U_R and U_L are the received and local oscillator (LO) fields, respectively, measured in the detector plane, $U_R(x_m,y_n,t)=|U_R(x_m,y_n,t)|\exp[-j\theta(x_m,y_n,t)]$, and the integration is performed over A_d, the area of the m,n-th detector. The local oscillator is assumed to be stabilized in frequency and assumed to produce a uniform plane wave so that $U_L(x_m,y_n t)=U_L$. Assuming that $\theta(x,y,t)$ does not vary over the area of an individual detector, factoring out

$\int_{A_d} |U_R(x_m,y_n,t)|^2+|U_L|^2 dx_m dy_n$ and defining:

$$i_{mn} = \frac{\eta}{hf_0} \int_{A_d} (|U_R(x_m,y_n,t)|^2+|U_L|^2) dx_m dy_n \tag{4}$$

$$= \frac{\int_{A_d} 2|U_R(x_m,y_n,t)| \cdot |U_L| dx_m dy_n}{\int_{A_d} |U_R(x_m,y_n,t)|^2+|U_L|^2 dx_m dy_n} \tag{5}$$

reduces equation (3) to:

$$i_{mn}(t) = i_{mn}\left[1+\gamma\cos(2\pi f_{IF}t+\theta_{mn}(t))\right] \tag{6}$$

Call γ the modulation index and i_{mn} the amplitude. It is easily seen that $\gamma \leq 1$. Since only one detector is being examined henceforth, the notation will be simplified by replacing i_{mn} with i_s and $\theta_{mn}(t)$ with $\theta(t)$. Equation (6) is the signal model which acts as the input to the preprocessor structure (integrate-and-dump filters) imposed by the CCD's.

There is an inferent uncertainty in the exact arrival and conversion times of incident photons at any particular detector imposed by the statistical nature of light. These uncertainties are known to result in a noise process associated with the signal that is Poisson distributed (Ref.5:53). However, if the arrival times of the photons are sufficiently close together, then for any finite bandwidth detector, the central limit theorem forces the resulting filtered statistics to be gaussian. (Ref.3:124). The smaller the bandwidth for a given arrival rate, the more closely the resulting process approximates a gaussian distribution. For typical local

oscillator power levels, the average photon arrival rate is so high that even relatively wideband detectors will exhibit gaussian statistics at their outputs (Ref.12). For the low bandwidth (compared to photoconductive or photovoltaic devices) CCD devices considered in this paper, the gaussian assumption is extremely good for local oscillator noise limited cases.

Preprocessor Structure

The output of a heterodyne detector with noise corruption is:

$$r(t) = h(t)+n(t) = i_s\left[1+\gamma \cos(2\pi f_{IF}t+\theta(t))\right]+n(t) \qquad (7)$$

where $h(t)$ is the phase modulated carrier, $\theta(t)$ is the phase process to be estimated, and $n(t)$ is a white, gaussian, zero mean noise process which accounts for the detector noise. Since $r(t)$ is the output of a total power detector, it clearly can never be negative. But, if $n(t)$ is truely gaussian, then there is a finite probability that it will take on values such that $r(t)$ does indeed become negative. The resolution of this apparent contradiction lies in the fact that $n(t)$ is never precisely gaussian. The noise $n(t)$ arises as a result of the fact that the photon arrival times are not known exactly, even if the field is deterministic and known. For a field with intensity (power at the detector plane) $I(t)$, the detector output will be

$r(t) = \alpha I(t)+n(t)$, where α is a constant of proportionality. It can be shown that the signal $r(t)$ is a Poisson process with rate parameter $\alpha I(t)$ (Ref.5:53). The mean of the process is given by $\alpha I(t)$ and so is the variance. The central limit theorem requires that, with a finite bandwidth detector, as the number of photoelectron conversions per second approaches infinity, the variable $(r(t)-\alpha I(t))/\sqrt{\alpha I(t)}$ will become gaussian with zero mean and unit variance (Ref.3:124). That is, $r(t)$ becomes gaussian with mean $\alpha I(t)$ and variance $\alpha I(t)$, hence, $n(t)$ becomes gaussian with mean zero and variance $\alpha I(t)$. However, the photon count per second approaches infinity only if $I(t)$ becomes infinite. This would force the mean and variance of $r(t)$ to infinity as well. For a large (but finite) photon arrival rate, the process will becomes very close to gaussian around the mean, but cannot be accurately modeled as gaussian far into the "tails". This is so since a Poisson process is defined only for (discrete) positive arguments, the process $r(t)$, a Poisson process, is defined only for values of its pdf greater than zero. That is, $f_{r(t)}(r(t))=0$ for $r(t)<0$. Therefore, the probability of $n(t)$ taking on values less than $-\alpha I(t)$ is zero, and $n(t)$ is not truely gaussian. Since $\alpha I(t)$ is very large, the truncation of the tails occurs at a very large number of standard deviations from the mean for even moderate intensities. Hense, the assumption that $n(t)$ is zero mean

and gaussian is very good for large fields incident on the detector (many photo electron conversions per second compared to the bandwidth of the detector). See Davenport and Root (Ref.3:124) and Karp and Gagliardi (Ref.5:130).

The effect of using a CCD detector is to introduce an integrate-and-dump filtering (IDF) on the signal before reaching any of the receiver electronics at the IF stage. The integration period of the CCD is user controlable as long as it is more than a certain minimum value set by the device characteristics. A typical minimum value might be 0.1μsec (Ref.2). Designate the number of integration periods per period of the IF by P_t . The output of the IDF is a sequence of random variables with the form:

$$r_i = \int_{-\frac{T}{2P_t}+\frac{T}{P_t}(i-1)+2\pi m(i-1)}^{-\frac{T}{2P_t}+\frac{T}{P_t}(i)+2\pi mi} r(t)dt$$

$$= \int_{\frac{T}{P_t}(i=\frac{3}{2})+2\pi m(i-1)}^{\frac{T}{P_t}(i-\frac{1}{2})+2\pi mi} h(t) + n(t)\, dt \qquad (8)$$

where $T=1/f_{IF}$. The factor of $-T/2P_t$ occurs in the integration limits in order to take advantage of trigonometric simplifications that result. The factors of $2\pi m$ are

included in the limits to indicate that it is not necessary to integrate over just one IF period. Since the IF period, T, is typically on the order of 20 ns or less, and the CCD connot integrate for less than a few tenths of a μsec, the CCD will obviously integrate for more than T/P_t seconds per sample. Since $h(t)$ is 2π- periodic, adding a factor of $2\pi m$ in the limits does not change the samples except that the variances of the outputs of the CCD's are reduced by the additional integration time and the constant bias (due to integrating i_s) is increased deterministically. Throughout this paper, m is set to zero simply for convenience. If $m \neq 0$, the restriction on the upper limit to the bandwidth of the process $\theta(t)$, to be imposed shortly, will be more stringent. As shown in equation (8), the sequence $\{r_i\}$ is the sum of a signal sequence $\{h_i\}$ and a noise sequence $\{n_i\}$. The output of the detector is observed for a total of K IF periods, the length of the observation interval is KT second and the length of the observation vector is KP_t elements. If $m \neq 0$, the total observation interval is $K(mP_t+1)T$. The observation vector is composed of K subvectors each of P_t elements:

$$\underline{r} = (r_1, r_2, \ldots, r_{P_t}; r_{P_t+1}, \ldots, r_{2P_t}; \ldots; r_{(K-1)P_t+1}, \ldots, r_{KP_t})^T \qquad (9)$$

$$= (\underline{r}_1, \underline{r}_2, \ldots, \underline{r}_K)^T \qquad (10)$$

The parameter P_t has been left as an arbitrary integer. If there is a value of P_t that minimizes the mean-squared error of the processor, that would be the optimum value of P_t to use in a processor. To determine if such a value exists and what that value is, a Cramer-Rao (CR) lower bound is computed.

Cramer-Rao Lower Bound

The CR lower bound for the unbiased estimate of a parameter ζ is given by (Ref.17:66):

$$E\left[(\zeta-\hat{\zeta})^2\right] \geq \varepsilon^2 = -E\left[\frac{\delta^2}{\delta\zeta^2} \ln f(\underline{r}|\zeta)\right]^{-1} \qquad (11)$$

where $\hat{\zeta}$ is the estimate of the parameter, $\underline{r}$ is the total observation vector, $f(\underline{r}|\zeta)$ is the probability density function (pdf) or $\underline{r}$ conditioned on knowing the true value ζ, and $E[]$ is the expectation operator. The conditional pdf $f(\underline{r}|\theta(t))$ is required. The signal is a deterministic function of the phase and the noise is assumed to be independent of the phase. Since the noise is additive, $f(\underline{r}|\theta(t))$ is just $f(\underline{n})$ shifted to a mean value of $\underline{h}$.

Since $n(t)$ is white and gaussian, and the integral is a linear operator, integrated samples of $n(t)$ will form a gaussian sequence. It is easily derived that $\{n_i\}$ is a

white and zero mean sequence, as well.

$$E\left[n_i\right] = E\left[\int n(t)dt\right] = \int E\left[n(t)\right] dt = 0 \tag{12}$$

$$E\left[n_i n_j\right] = E\left[\int_i n(t)dt \int_j n(t')dt'\right] \tag{13}$$

$$= \iint E\left[n(t)n(t')\right]dtdt' = \iint \frac{N_0}{2}\delta(t-t')dtdt' \tag{14}$$

$$= \frac{N_0 T}{2P_t}\,\delta_{ij} \tag{15}$$

The two-sided spectral density of $n(t)$ has been denoted $N_0/2$. The appearance of the Kroenecker delta, δ_{ij} , demonstrates that the sequence is white, as expected. The pdf on $\underline{n}$ can now be written directly:

$$f(\underline{n}) = \left(\frac{2P_t}{\sqrt{2\pi}N_0 t}\right)^{P_t K} \exp\left[-\frac{1}{2}\cdot\frac{2P_t}{N_0 T}\cdot n^2\right] \tag{16}$$

Similarly, the conditional pdf of $\underline{r}|\theta(t)$ is:

$$f(\underline{r}|\theta) = \left(\frac{2P_t}{\sqrt{2\pi}N_0 T}\right)^{P_t K} \exp\left[-\frac{1}{2}\cdot\frac{2P_t}{N_0 T}\sum_{i=1}^{P_t K}(r_i-h_i)^2\right] \tag{17}$$

From equation (11) the CR bound is:

$$\varepsilon^2 = -E\left[\frac{\delta^2}{\delta\theta^2}\left(-\frac{P_t}{N_0 T}\sum(r_i-h_i)^2\right)\right]^{-1} \tag{18}$$

$$= \left[\frac{2P_t}{N_0 T}\sum\left(\frac{\delta h_i}{\delta\theta}\right)^2\right]^{-1} \qquad (19)$$

Where the fact that $\mathbf{E}[r_i] = h_i$ was exploited (since $n(t)$ is zero mean) to remove the term involving the second derivative of h_i. Inserting equation (6) into equation (8) gives:

$$h_i(\theta(t_i)) = \frac{i_s T\gamma}{2\pi}\left[\cos\left(\frac{2\pi}{P_t}(i-\tfrac{1}{2})+\theta(t_i)\right)-\cos\left(\frac{2\pi}{P_t}(i-\frac{3}{2})+\theta(t_i)\right)\right] \qquad (20)$$

where $t_i = T(i-\frac{1}{2})/P_t$. It was also assumed in this integral that $\theta(t)$ does not change over the period of integration, else the integration could not be performed without explicit knowledge of the functional form of $\theta(t)$, if then. Furthermore, if the phase changes much over one measurement interval, then some sort of average of the phase over the interval will be estimated. Consequently, it will be assumed that the bandwidth of the process $\theta(t)$ is small enough that the realization being examined changes very little over the measurement interval, with high probability. Equivalently, some statistical measure of the bandwidth of the phase process is assumed known a-priori and the measurement interval is chosen so that the phase process realization will change by less than some small, predetermined bound during the measurement interval with some high degree of probability chosen by the designer. If the m in equation (8) is

large, this can be a rather stringent condition.

With these assumptions, the CR bound becomes:

$$\varepsilon^2 = \frac{N_0}{2T}\left(\frac{2\pi}{i_s\gamma}\right)^2 \left\{ P_t \sum \left[\cos(x_i)-\cos\left(x_i-\frac{2\pi}{P_t}\right)\right]^2 \right\}^{-1} \qquad (21)$$

$$x_i = \frac{2\pi}{P_t}(i-1) + \theta_i \qquad (22)$$

Using the trigonometric identity for cos(x)-cos(y) and applying the results of Appendix A to the summation results in:

$$\varepsilon^2 = \frac{N_0}{2T}\left(\frac{2\pi}{i_s\gamma}\right)^2 \left[2P_t^{\,2}\cdot K\cdot \sin^2\left(\frac{\pi}{P_t}\right)\right]^{-1} \qquad (23)$$

$$\varepsilon^2 = \left[\frac{N_0}{2TK}\cdot\frac{2}{(i_s\gamma)^2}\right]\cdot\frac{\pi^2}{P_t^2\,\sin^2(\pi/P_t)} \qquad (24)$$

As $P_t \to \infty$, this equation reduces to $\varepsilon^2 = \frac{N_0}{2KT}\cdot\frac{2}{(i_s\gamma)^2}$ which is the same as the error for the linearized first order PLL (Ref.18:93), or the CR bound for a system which has access to the non-integrated, non-sampled waveform. For P_t finite, the error bound will be greater than that for the PLL by a factor of $\pi^2/P_t^2\,\sin^2(\frac{\pi}{P_t})$. In all simulations, P_t= 4 simply to reduce computer time requirements. For larger P_t , an appropriate scale factor can be introduced into the simulated errors by using equation (24).

III. Processor Determination: Maximum Likelihood Estimation

Three specific cases of the estimation problem can be identified:

(i) $\theta(t)$ is a constant, θ_0, for all time. It may be construed as a single realization of a random variable uniformly distributed between $-\pi$ and π radians.

(ii) $\theta(t)$ is a random process with unknown statistics.

(iii) $\theta(t)$ is a random process with known statistics.

The first two cases are analyzed in this chapter and it is shown that the optimum processor is a discretized phase-locked loop. Because of the nature of the integrate-and-dump preprocessing imposed on the measurements, it may not be obvious that the optimum ML processor still has a PLL structure. The third case is analyzed in the next chapter.

Measurement Model Equations

Before continuing, it is convenient to derive the exact form of $h_i(\theta)$ and its first two derivatives with respect to θ. Using equation (6) in equation (8) gives $h_i(\theta)$, which can be differentiated directly.

$$h_i(\theta) = i_s T\left[\frac{1}{p_t} + \frac{\gamma}{\pi}\sin(\frac{\pi}{p_t})\cos(\frac{2\pi}{p_t}(i-1)+\theta)\right] \qquad (25)$$

$$\frac{\delta h_i(\theta)}{\delta\theta} = -\frac{i_s T\gamma}{\pi}\sin(\frac{\pi}{P_t})\sin(\frac{2\pi}{P_t}(i-1)+\theta) \tag{26}$$

$$\frac{\delta^2 h_i(\theta)}{\delta\theta^2} = -\frac{i_s T\gamma}{\pi}\sin(\frac{\pi}{P_t})\cos(\frac{2\pi}{P_t}(i-1)+\theta) \tag{27}$$

These equations are used many times in the derivations that follow and will be referred to quite often. These equations are needed because the first derivative is always necessary in the derivation of the ML processor. The second derivative will be used when the Kalman filter is derived because the nonlinear measurements will be linearized in a Taylor series expansion and the second derivative appears in the derivation.

Maximum Likelihood Approach: Case (i)

The ML estimate of θ_0 is the value of θ_0 that maximizes the conditional density $f(\underline{r}|\theta_0)$. Since $f(\underline{r}|\theta_0)$ is gaussian, the ML estimate is the value of θ_0 , $\hat{\theta}_0$, that solves:

$$\frac{\delta}{\delta\theta_0}\ln f(\underline{r}|\theta_0) = 0 \tag{28}$$

Taking the logarithm of equation (17) and differentiating gives:

$$\sum_{i=1}^{KP_t}(r_i-h_i)\frac{\delta h_i}{\delta\theta_0} = 0 \tag{29}$$

Inserting equations (26) and (27) results, after some trigonometric identities are applied:

$$0 = \sum r_i \sin\left(\frac{2}{P_t}(i-1)+\theta_0\right) - \sum \frac{i_s T}{P_t} \sin\left(\frac{\pi}{P_t}\right)\sin\left(\frac{2\pi}{P_t}(i-1)+\theta_0\right)$$

$$- \sum \frac{\gamma i_s T}{2\pi} \sin\left(\frac{\pi}{P_t}\right) \sin\left(\frac{4\pi}{P_t}(i-1)+2\theta_0\right) \qquad (30)$$

The trigonometric terms in the last two summations are shown to sum to zero in Appendix A. The estimator reduces to:

$$\sum_{i=1}^{KP_t} r_i \sin\left(\frac{2\pi}{P_t}(i-1)+\hat{\theta}\right) = 0 \qquad (31)$$

This processor is a discrete analog to the familiar PLL and can be implemented in closed loop form for any values of K and P_t. A block diagram is shown in Figure 2. The dotted box encloses a discrete IDF(DIDF).

Maximum Likelihood Approach: Case (ii)

Suppose that $\theta(t)$ is not constant over the entire observation interval. In light of Appendix A, let the phase be approximately constant over one period, T, but vary from period to period in an unknown manner. Equation (31) becomes:

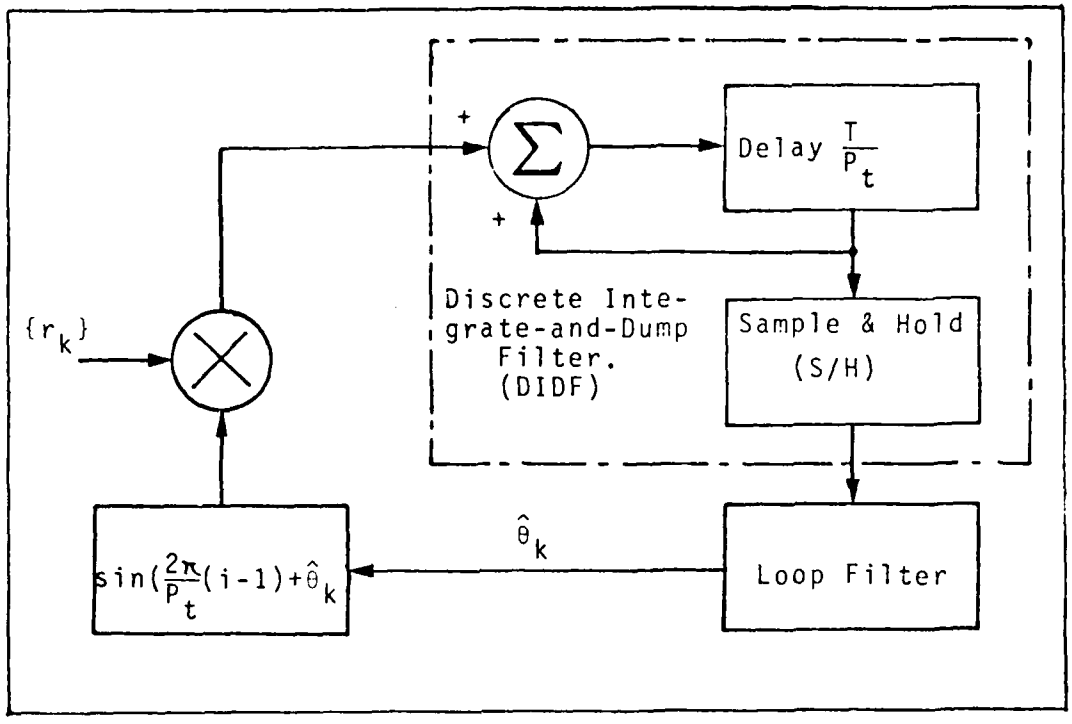

Figure 2. Maximum Likelihood Estimator

$$\sum_{m=1}^{K} \sum_{i=1}^{P_t} r_{im} \sin(\frac{2\pi}{P_t}(i-1)+\hat{\theta}_m) = 0 \qquad (32)$$

If equation (32) is to be true for any value of K, then the inner sum must be zero for every m. The estimator is then:

$$\sum_{i=1}^{P_t} r_i \sin(\frac{2\pi}{P_t}(i-1)+\hat{\theta}_m) = 0 \qquad (33)$$

The estimator produces a sequence of estimates, $\{\hat{\theta}_m\}$. As might be expected, θ_m is estimated independently of any past value of $\hat{\theta}_m$ or θ_m and only data from the current measurement interval $[mT, (m+1)T]$ is used to perform the estimation. That is, $\underline{r}=(r_1, r_2, \ldots, r_{P_t})^T$. This is directly a result of the fact that $\{\theta_k\}$ is (or is assumed to be) an uncorrelated sequence: $E[\theta_k \theta_l]=K_\theta \delta_{kl}$.

IV. Processor Determination: State Variable Analysis and Kalman Filtering

If some information concerning the time correlation of the process $\theta(t)$ is already known, it should be possible to obtain a better estimate (lower variance estimate) of the process by incorporating the a-priori information into the processor. In this chapter, state variable models and nonlinear Kalman filtering are applied to the problem of incorporating a-priori information into the processing algorithm. A few words are said about state variable equations in general and then the arguments are specialized for the measurement model of interest.

State Variable Equations

The phase process is assumed to be the output of a linear, time invariant system driven by white gaussian noise. This system is described by n state variables in a vector differential equation (Ref.13:556).

$$\dot{\underline{x}}(t) = F\,\underline{x}(t) + G\underline{u}(t) \tag{34}$$

$$\theta(t) = \underline{c}^T\,\underline{x}(t) \tag{35}$$

$$\underline{c}^T = (0,0,\ldots,0,1) \tag{36}$$

where:

$\underline{x}(t)$ n-dimensional state vector

$\underline{u}(t)$ m-dimensional noise vector

F nxn-dimensional system matrix

G nxm-dimensional noise system matrix

The solution to equation (34) is (Ref.13:556):

$$\underline{x}(t) = \phi(t-t_0)\underline{x}(t_0) + \int_{t_0}^{t} \phi(t-t')G\underline{u}(t')dt' \qquad (37)$$

Where $\phi(t-t_0)$ is called the system transition matrix and solves equation (38) with initial condition (39)(Ref.13:557):

$$\dot{\phi}(t-t_0) = F\phi(t-t_0) \qquad (38)$$

$$\phi(0) = I \qquad (39)$$

Since the data to be processed is discrete, a discrete formulation of equation (37) is:

$$\underline{x}(kT) = \underline{x}_k = \left[\phi(T)\right]^k \underline{x}_0 + \sum_{l=0}^{k-1} \left[\phi(T)\right]^{k-l} G\ \underline{u}_l \qquad (40)$$

This equation can be put into a recursive form with only moderate algebraic manipulation (Ref.13:557):

$$\underline{x}_k = \phi\underline{x}_{k-1} + \phi G\ \underline{u}_{k-1} \qquad (41)$$

For the time invariant case, the solution to equation (38) is $\exp(F(t-t_0))=\phi(t-t_0)$ which becomes, for discrete measurements (Ref.13:558):

$$\phi = \phi(T) = \exp\left[FT\right] \tag{42}$$

It will now be assumed that the phase does not change during an IF period (or changes very little) so that the phase process is described by a sequence of random variables $\{\theta_k\}$ or, alternatively, $\{\underline{x}_k\}$, where the variables are separated by T seconds. This will allow taking advantage of the trigonometric simplifications proven in Appendix A.

$$\underline{r}_k = \underline{h}(\theta_k) + \underline{n}_k = \underline{h}(\underline{c}^T\underline{x}_k) + \underline{n}_k \tag{43}$$

Where $\underline{n}_k$ is a white, gaussian vector with statistics:

$$E\left[\underline{n}_k\right] = \underline{0} \qquad E\left[\underline{n}_k\underline{n}_l^T\right] = R\delta_{kl} = \frac{N_0T}{2P_t}\cdot I\cdot\delta_{kl} \tag{44}$$

The dimensionality of $\underline{r}$, $\underline{h}$, and $\underline{n}$ is P_t. The matrix I is a $P_t x P_t$ identity matrix. The sequence $\{\underline{u}_k\}$ is white and gaussian with covariance matrix Q. The sequences $\{\underline{n}_k\}$ and $\{\underline{u}_k\}$ are independent. These assumptions, plus the initial conditions are:

$$E\left[\underline{u}_k\right] = \underline{0} \qquad E\left[\underline{u}_k\underline{u}_l^T\right] = Q\delta_{kl} \tag{45}$$

$$E\left[\underline{u}_k\underline{u}_l^T\right] = 0 \qquad E\left[\underline{x}_k\underline{u}_l^T\right] = \text{[illegible]} \tag{46}$$

$$E\left[\underline{x}_0\right] = \overline{\underline{x}}_0 \qquad E\left[(\underline{x}-\underline{x}_0)(\underline{x}-\underline{x}_0)^T\right] = P_0 \tag{47}$$

Given the received sequence $\{\underline{r}_k\}$, an "optimum" estimate of the state $\{\hat{\underline{x}}_k\}$ is desired from which an optimum estimate of the phase $\{\hat{\theta}_k\}=\{\underline{c}^T\hat{\underline{x}}_k\}$ can be derived, or any other element of the state vector. Unfortunately, no general solution to this problem exists for arbitrary nonlinear functions $\underline{h}(\cdot)$ in either the continuous or discrete case. Exact solutions do exist for linear $\underline{h}(\cdot)$ and approximate solutions do exist for a nonlinear $\underline{h}(\cdot)$ which has been linearized by a Taylor series expansion about the best estimate of the state, $\hat{\underline{x}}_k$. Sage solves the problem using a discrete invariant embedding procedure (Ref.14: 450) to give the equations for a maximum a-posteriori (MAP) estimate:

$$\underline{r}_k = \underline{h}\ (\underline{x}_k)+\underline{n}_k \tag{48}$$

$$\hat{\underline{x}}_{k+1} = \phi\hat{\underline{x}}_k + P_{k+1}\phi^{-T}\ \frac{\delta}{\delta\hat{\underline{x}}_k}\ \underline{h}^T(\phi\hat{\underline{x}}_k)R_k^{-1}\left[\underline{r}_{k+1}-\underline{h}(\phi\hat{\underline{x}}_k)\right] \tag{49}$$

$$P_{k+1} = P_k'\left[\phi^{-T}-\phi^{-T}\left\{\frac{\delta}{\delta\hat{\underline{x}}_k^T}\left[\ \frac{\delta}{\delta\hat{\underline{x}}_k}\ \underline{h}^T(\phi\hat{\underline{x}}_k)R^{-1}\left\{\underline{r}_{k+1}-\underline{h}(\phi\hat{\underline{x}}_k)\right\}\right]\right\}\phi^{-1}P_k'\right]^{-1} \tag{50}$$

$$P_k' = \phi P_k + GQG^T\phi^{-T} \tag{51}$$

When $\underline{h}(\phi\hat{\underline{x}}_k)=\underline{h}(\underline{c}^T\phi\hat{\underline{x}}_k)=\underline{h}(\hat{\theta}_k')$, this can reduce to (see Appendix B):

$$\underline{r}_k = \underline{h}(\theta_k) + \underline{n}_k \tag{52}$$

$$\underline{\hat{x}}_{k+1} = \phi\underline{\hat{x}}_k + P_{k+1}\underline{c}\,\frac{\delta\underline{h}^T(\hat{\theta}_k')}{\delta\hat{\theta}_k'}\,R^{-1}\left[\underline{r}_{k+1} - \underline{h}(\hat{\theta}_k')\right] \tag{53}$$

$$P_{k+1} = P_k'\left[\phi^{-T} - \underline{c}\left\{\frac{\delta^2\underline{h}^T(\hat{\theta}_k')}{\delta\hat{\theta}_k'^2}\,R^{-1}\left[r_{k+1} - \underline{h}(\hat{\theta}_k')\right] - \frac{\delta\underline{h}^T(\hat{\theta}_k')}{\delta\hat{\theta}_k'}\,R^{-1}\,\frac{\delta\underline{h}(\hat{\theta}_k')}{\delta\hat{\theta}_k'}\right\}\underline{c}^T P_k'\right]^{-1} \tag{54}$$

$$P_k' = \phi P_k + GQG^T\phi^{-T} \tag{55}$$

$$\hat{\theta}_k' = \underline{c}^T\phi\underline{\hat{x}}_k \tag{56}$$

Appendix B further specializes for the measurement model given in equations (25)-(27). The results are:

$$\underline{\hat{x}}_{k+1} = \phi\underline{\hat{x}}_k - \frac{1}{\sigma_n^2}\cdot\frac{i_s^T\gamma}{\pi}\cdot\sin\left(\frac{\pi}{P_t}\right)\cdot P_{k+1} - \underline{c}$$

$$\sum_{i=1}^{P_t}\underline{r}_{k+1}(i)\sin\left(\frac{2\pi}{P_t}(i-1)+\hat{\theta}_k'\right) \tag{57}$$

$$P_{k+1} = \left[(\phi P_k \phi^T + Q')^{-1} + \underline{c}\underline{c}^T \frac{i_s^T \gamma}{\pi \sigma_n^2} \cdot \sin(\frac{\pi}{P_t}) \right.$$

$$\left. \sum_{i=1}^{P_t} \underline{r}_{k+1}(i) \cos(\frac{2\pi}{P_t}(i-1)+\hat{\theta}_k') \right]^{-1} \qquad (58)$$

$$Q' = GQG^T \qquad \sigma_n^2 = \frac{N_0 T}{2P_t} \qquad (59)$$

Letting $\underline{r}_k = \underline{h}(\theta_k) + n_k$ (where θ_k is the actual angle) and substituting equation (25) for $\underline{h}(\theta_k)$ and utilizing the relations proved in Appendix A gives (see Appendix B):

$$\hat{\underline{x}}_{k+1} = \phi \hat{\underline{x}}_k - (P_{k+1}\underline{c}) \cdot \frac{\sqrt{2}P_t}{\pi} \cdot \sin(\frac{\pi}{P_t}) \cdot CNR \sum_{i=1}^{P_t} z_{k+1}(i)$$

$$\sin(\frac{2\pi}{P_t}(i-1)+\hat{\theta}_k') \qquad (60)$$

$$P_{k+1}^{-1} = (\phi P_k \phi^T + Q')^{-1} + \underline{c}\underline{c}^T \cdot \frac{\sqrt{2}P_t}{\pi} \cdot \sin(\frac{\pi}{P_t}) \cdot CNR \cdot \sum z_{k+1}(i)$$

$$\cos(\frac{2\pi}{P_t}(i-1)+\hat{\theta}_k') \qquad (61)$$

where:

$$CNR = \frac{(i_s\gamma)^2}{2} \Big/ \frac{N_0}{2T} \tag{62}$$

$$z_{k+1}(i) = \frac{i_s\gamma}{\pi} \sin(\frac{\pi}{P_t})\cos(\frac{2\pi}{P_t}(i-1)+\theta_{k+1})+n'_{k+1}(i) \tag{63}$$

$$\sigma_{n'}^2 = \frac{N_0}{2P_tT} \tag{64}$$

The carrier-to-noise ratio (CNR) thus defined is the ratio of the signal power to the noise power in the total bandwidth used in producing the estimate (1/T) . This is the same CNR used by Viterbi (Ref.18:93) and thus allows direct comparisons with his results for the PLL. In addition, the CNR gives an intuitive feel for how "good" the measurements are, or how badly they are corrupted by measurement noise.

Processor Ambiguity

Appendix B shows that the processor equations can be further simplified to:

$$\hat{\underline{x}}_{k+1} = \phi\hat{\underline{x}}_k - P_{k+1}\,\underline{c}\left[\beta\cdot\sin(\theta_{k+1}-\hat{\theta}'_k) + n_{ks}\right] \tag{65}$$

$$P_{k+1}^{-1} = \left[\phi P_k \phi^T+Q'\right]^{-1} + \underline{c}\,\underline{c}^T\left[\beta\cdot\cos(\theta_{k+1}-\hat{\theta}'_k)+n_{kc}\right] \tag{66}$$

where:

$$\beta = \frac{p_t^2}{\pi^2} \cdot \sin^2\left(\frac{\pi}{P_t}\right) \cdot CNR \tag{67}$$

$$\text{var}\left[n_{ks}\right] = \text{var}\left[n_{kc}\right] = \beta \qquad E\left[n_{ks}n_{kc}\right] = 0 \tag{68}$$

The sequences $\{n_{ks}\}$ and $\{n_{kc}\}$ are also zero mean. For any plant model which is one dimensional, $\underline{x}_k = x_k = \theta_k$ and $\underline{c}\underline{c}^T = 1$. For this case, plugging equation (66) into (65), assuming the noise is negligible, and dividing top and bottom by $\cos(\theta_{k+1} - \hat{\theta}_k')$:

$$\hat{\theta}_{k+1} = \hat{\theta}_k' - \frac{\tan(\theta_{k+1} - \hat{\theta}_k')}{\beta^{-1}(\phi P_k \phi^T + Q')^{-1}\sec(\theta_{k+1} - \hat{\theta}_k') + 1} \tag{69}$$

For large CNR, the estimate should be quite good and, within modulo-2π, $\theta_{k+1} - \hat{\theta}_k' \simeq 0$. Since $\sec(0) = 1$, equation (69) reduces to, approximately:

$$\hat{\theta}_{k+1} = \hat{\theta}_k' - \frac{1}{1 + \beta^{-1}(\phi P_k \phi^T + Q')^{-1}} \cdot \tan(\theta_{k+1} - \hat{\theta}_k') \tag{70}$$

However, the function $\tan(\cdot)$ exhibits a modulo-π ambiguity, so that $\tan(\theta_{k+1} - (\hat{\theta}_k' \pm p\pi)) = \tan(\theta_{k+1} - \hat{\theta}_k')$, where p is any integer. Thus, the estimator will be unable to determine the phase better than modulo-π .

The above arguments were for a one-dimensional state

vector with high CNR. Simulations have confirmed this result for smaller CNR's as well.

Constant Phase

The case of a constant phase plant is the simplest case to model. The state vector has but one component and the matrices collapse to scalars. The state variable equations become:

$$\theta_{k+1} = \theta_k \tag{71}$$

$$\phi = 1 \qquad G = 0 \qquad R = \frac{N_0 T}{2P_t} \qquad Q = \text{arbitrary} \tag{72}$$

The estimator or Kalman filter equations are, from (65) and (66):

$$\hat{\theta}_{k+1} = \hat{\theta}_k - P_{k+1}\left[\beta \cdot \sin(\theta - \hat{\theta}_k) + n_{ks}\right] \tag{73}$$

$$P_{k+1}^{-1} = P_k^{-1} + \left[\beta\cos(\theta - \hat{\theta}_k) + n_{kc}\right] \tag{74}$$

Figure (3b) is a block diagram of this processor. Figure (3a) shows the processor in the form given by equations (57) and (58).

Random Phase Walk

The random walk is modelled by the state variable equation:

$$\theta_{k+1} = \theta_k + Gu_k \tag{75}$$

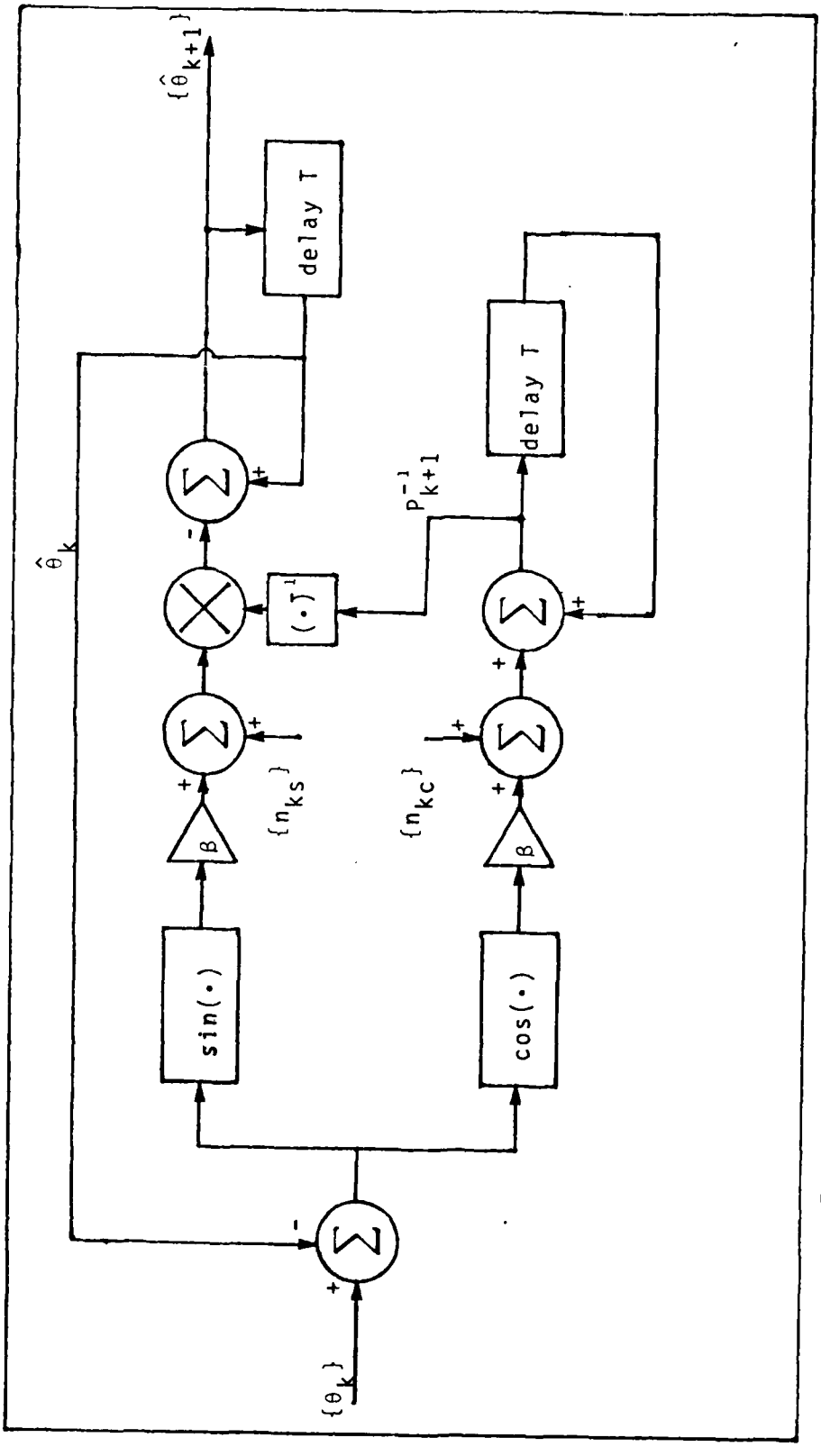

Figure 3a. Constant Phase Processor Structure (Realization 1).

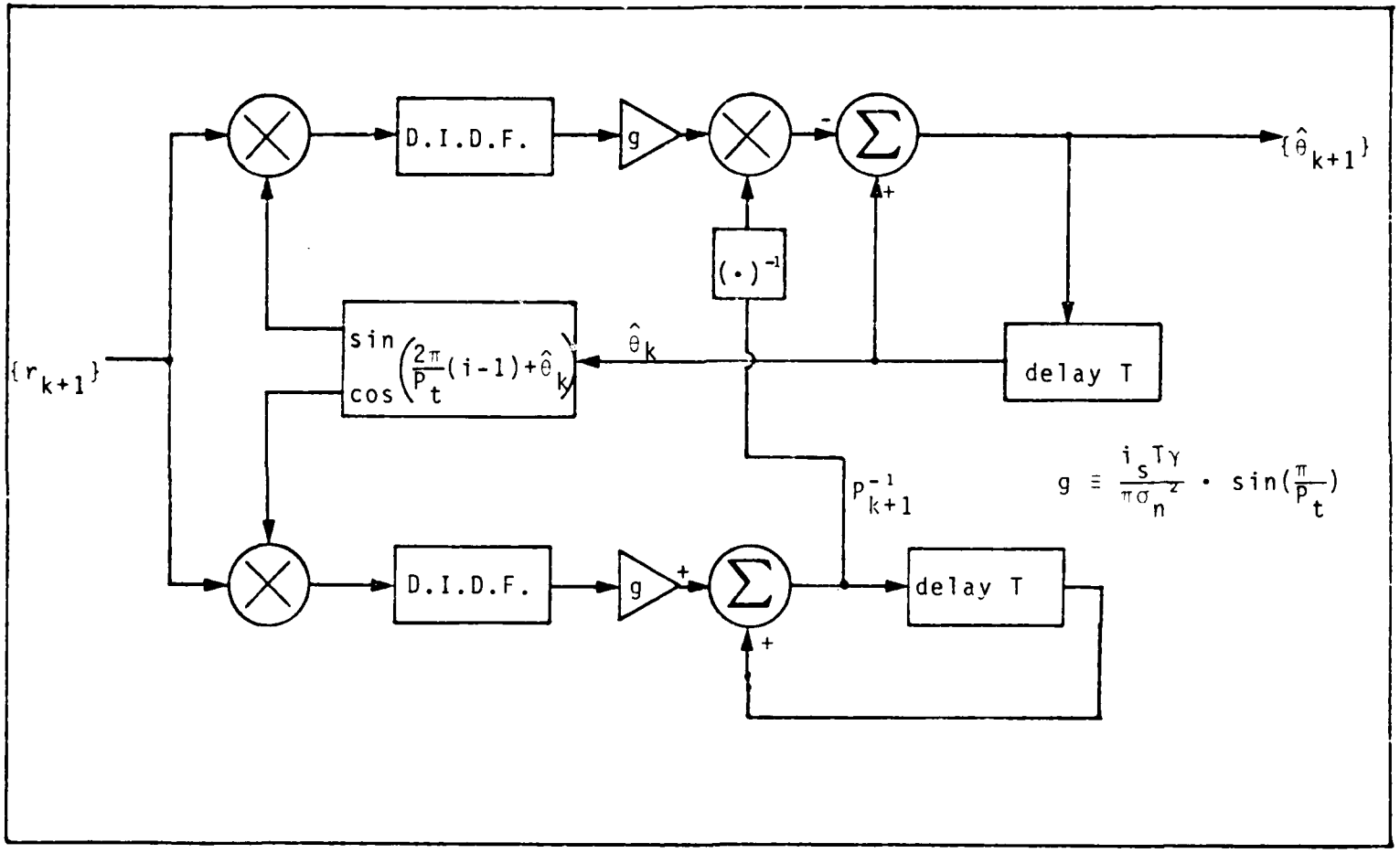

Figure 3b. Constant Phase Processor Structure (Realization 2)

Let var $\left[u_k\right]=Q=1$, for simplicity, so that the variance of the noise term is reflected in the value of G . Also, $\phi=1$, and $R=N_0T/2P_t$ as in the constant phase case. The filter equations are:

$$\hat{\theta}_{k+1} = \hat{\theta}_k - P_{k+1}\left[\beta\cdot\sin(\theta_{k+1}-\hat{\theta}_k')+n_{ks}\right] \tag{76}$$

$$P_{k+1}^{-1} = (P_k+G^2)^{-1} + \beta\cos(\hat{\theta}_{k+1}-\hat{\theta}_k')+n_{kc} \tag{77}$$

Figure (4b) shows this processor while Figure (4a) shows the implementation according to equations (57) and (58). Both forms of the filter are shown because while the form of equations (65) and (66) gives a good intuitive feel for how the filters process the estimation error, the form of equations (57) and (58) is the actual form a hardware processor would take. This is true because actual phase is quite clearly unavailable to the processor.

Demodulation of FM Signals

Suppose that the information of interest in a state vector is given by $m(t)=\underline{c}^T\underline{x}(t)$. Suppose also that the phase of the carrier is given not by $m(t)$, but by $\theta(t)=\lambda\int_0^t m(\tau)d\tau+\theta_0$ so that $\dot{\theta}(t)=m(t)=\lambda\underline{c}^T\underline{x}(t)$ where λ is called the frequency modulation index. A new state vector can be constructed from the old state vector and $\theta(t)$. The new state variable equation is:

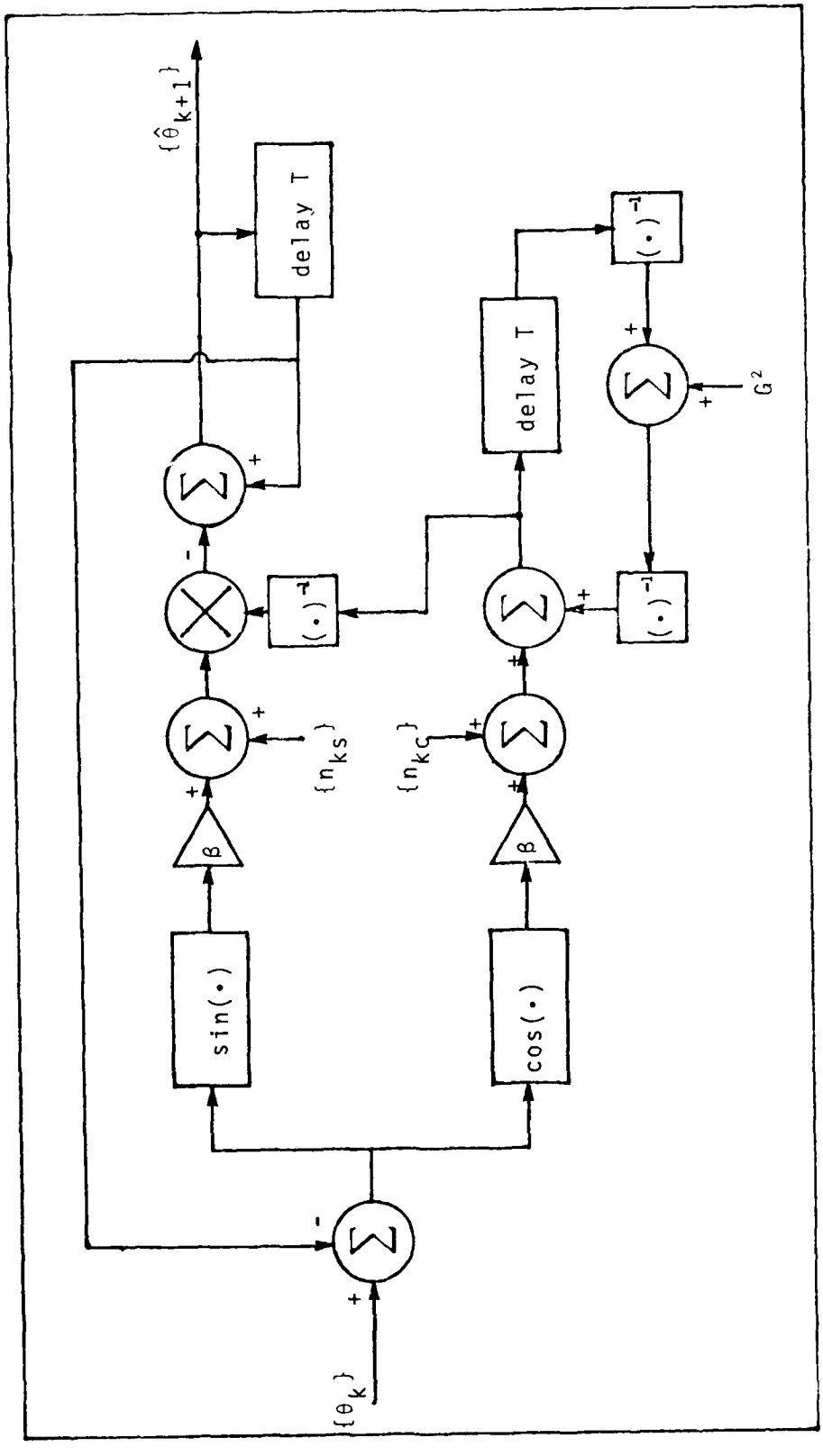

Figure 4a. Random Walk Processor Structure (Realization 1)

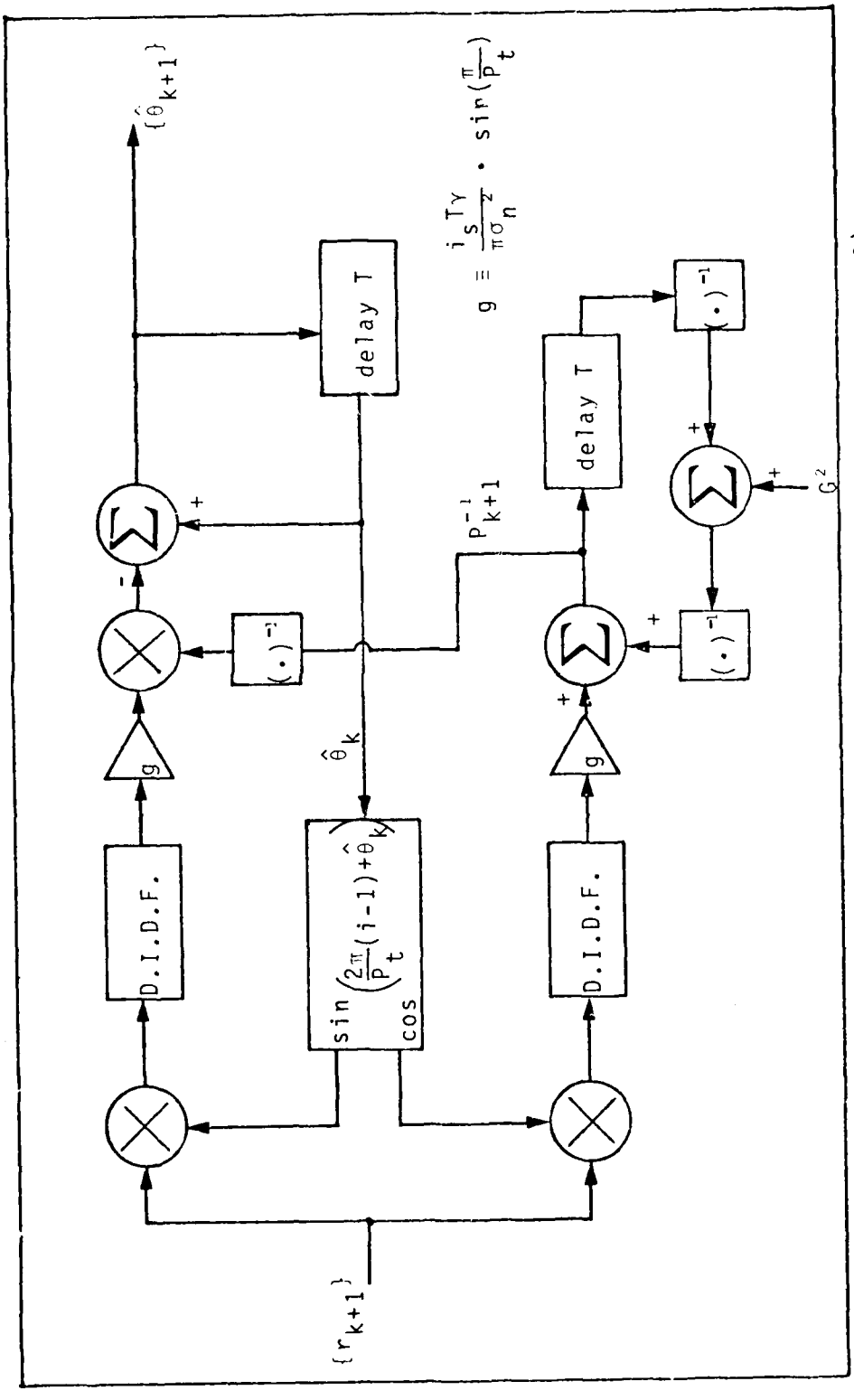

Figure 4b. Random Walk Processor Structure (Realization 2)

$$\dot{\underline{x}}\ (t) = \begin{bmatrix} \dot{\underline{x}}(t) \\ \dot{\theta}(t) \end{bmatrix} = \begin{bmatrix} F & 0 \\ \underline{c}^T\lambda & F_\theta \end{bmatrix} \begin{bmatrix} \underline{x}(t) \\ \theta(t) \end{bmatrix} + \begin{bmatrix} G & 0 \\ 0 & G_\theta \end{bmatrix} \begin{bmatrix} \underline{u}(t) \\ u_\theta(t) \end{bmatrix} \quad (78)$$

$$\dot{\underline{x}}'(t) = F'\ \underline{x}'(t) + G'\ \underline{u}'(t) \quad (79)$$

Where F_θ has been added to the F' matrix to account for possible variations in $\theta(t)$ not due to the FMing of the carrier by $m(t)$. In the discrete formulation:

$$\underline{x}'_{k+1} = \phi'\underline{x}'_k + \phi'G'\underline{u}'_k \quad (80)$$

$$\phi' = \exp\left[F'T\right] \qquad E\left[\underline{u}'_k\underline{u}'^T_1\right] = \begin{bmatrix} Q & 0 \\ 0 & Q_\theta \end{bmatrix}\delta_{kl} \quad (81)$$

The plant equation, and hence the filter equation, is at least two dimensional, but this is no theoretical complication.

A practical case is when the frequency is a constant over the observation interval. This could come up when estimating phase in the presence of an unknown doppler shift. Model the system with two state variables and suppose the phase, in the absence of the doppler shift, would be executing a random walk. Then:

$$\dot{\underline{x}}'(t) = \begin{bmatrix} 0 & 0 \\ \lambda & 0 \end{bmatrix} \begin{bmatrix} x(t) \\ \theta(t) \end{bmatrix} + \begin{bmatrix} 0 & 0 \\ 0 & G_\theta \end{bmatrix} \begin{bmatrix} u(t) \\ u_\theta(t) \end{bmatrix} \quad (82)$$

$$\underline{x}'_{k+1} = \begin{bmatrix} 1 & 0 \\ \lambda T & 1 \end{bmatrix} \begin{bmatrix} x_k \\ \theta_k \end{bmatrix} + \begin{bmatrix} 0 & 0 \\ 0 & G_\theta \end{bmatrix} \begin{bmatrix} u_k \\ u_{\theta k} \end{bmatrix} \tag{83}$$

$$= \phi' \underline{x}'_k + (\phi' G') \underline{u}'_k \tag{84}$$

The solutions to the problem, the filter equations, are:

$$\hat{\underline{x}}'_{k+1} = \phi' \hat{\underline{x}}'_k - P_{k+1} \underline{c} [\beta \sin(\theta_{k+1} - \hat{\theta}'_k) + n_{ks}] \tag{85}$$

$$P^{-1}_{k+1} = (\phi' P_k' \phi^T + G' Q'' G'^T)^{-1} + \underline{c}\, \underline{c}^T \beta \cos(\theta_{k+1} - \hat{\theta}'_k) + n_{kc} \tag{86}$$

where:

$$E[\underline{u}'_k \underline{u}'_l] = Q'' \delta_{kl} \qquad \hat{\theta}'_k = \underline{c}^T \phi' \hat{\underline{x}}'_k \tag{87}$$

It is now possible to estimate both phase and frequency. The doppler shift is given by $\hat{x}_{k+1} = \underline{d}^T \hat{\underline{x}}'_{k+1}$ and the phase is given by $\hat{\theta}_{k+1} = \underline{c}^T \hat{\underline{x}}'_{k+1}$, where $\underline{d}^T = (1,0)$.

Phase Estimation with Frequency Uncertainty

Imagine a case where it is desired to estimate the phase of an optical field, but the local oscillator is known to be unstable. Alternatively, the LO may be stable and the received field frequency fixed, but the integration limits may not be controlled precisely. The uncertainty in the limit times, $\frac{T}{P_t}(i-\frac{1}{2})$, can be modelled as an uncertainty in $f_{IF} = \frac{1}{T}$.

The frequency uncertainty can be incorporated into the model of equation (80) by simply allowing $G \neq 0$. Unfortunately, the state-variable models assume a driving force which is white, and the frequency uncertainty of a local oscillator is not even nearly white for any case of interest. The state-variable models can accomodate non-white driving functions by driving a "coloring filter" with white noise and allowing the output of the coloring filter to drive the system of interest. The state variable equations for the coloring filter are then used to augment the original state variable equation (Ref.7:180). The coloring filter is described by:

$$\dot{\underline{x}}_f(t) = F_f \underline{x}_f(t) + G_f \underline{u}_f(t) \tag{88}$$

$$\underline{u}(t) = H_f \underline{x}_f(t) \tag{89}$$

Where the notation in equation (89) is meant to indicate that only the $\underline{u}(t)$ portion of $\underline{u}'(t)$ in equation (79) is augmented while $u_\theta(t)$ (and, for that matter, any portions of $\underline{u}(t)$ that are already white) is not an output of the system $\underline{x}_f(t)$. The augmented system is described by:

$$\begin{bmatrix} \dot{\underline{x}}_f(t) \\ \dot{\underline{x}}(t) \\ \dot{\theta}(t) \end{bmatrix} = \begin{bmatrix} F_f & 0 & 0 \\ GH_f & F & 0 \\ 0 & \underline{c}^T\lambda & F_\theta \end{bmatrix} \begin{bmatrix} \underline{x}_f(t) \\ \underline{x}(t) \\ \theta(t) \end{bmatrix} + \begin{bmatrix} G_f & 0 \\ 0 & 0 \\ 0 & G_\theta \end{bmatrix} \begin{bmatrix} \underline{u}_f(t) \\ \underline{u}_\theta(t) \end{bmatrix} \tag{90}$$

$$\dot{\underline{x}}_a(t) = F_a \cdot \underline{x}_a(t) + G_a \cdot \underline{u}_a(t) \tag{91}$$

The discretized equation is given by:

$$\underline{x}_a(k+1) = \phi_a \underline{x}_a(k) + \phi_a G_a \underline{u}_a(k) \tag{92}$$

$$\phi_a = \exp\left[F_a T\right] \tag{93}$$

Where, for ease of reading, the subscript k has been replaced by the argument k. The filter equations are simply equations (65) and (66), or equations (57) and (58), with all quantities replaced by their associated augmented counterparts. Note carefully that $\underline{u}_a(t)$ is now a white process driving the augmented system. This is as far as it is possible to go without assuming certain correlations for $\underline{x}_f(t)$.

It is cautioned that it was assumed that $\theta(t)$ could be modelled as the output of a system driven by white noise. If this is not the case, then equation (89) is modified so that $\underline{u}(t) = H_f \underline{x}_f(t)$. Also, it was assumed that $\underline{u}(t)$ is the output of a system all of whose inputs were non-white. If this is not the case, then some elements of $\underline{u}(t)$ are not included in (89), are not augmented, and enter equation (90) in their original form. A further caution is that since the white noise driving function, $\underline{u}_f(t)$, is gaussian, the resulting density for $\underline{u}(t)$, the frequency

uncertainty, is also gaussian for any linear plant model. This is because a gaussian process remains gaussian after being transformed by a linear system. So, if a white, gaussian process $\underline{u}_f(t)$ drives a linear, time invariant system to produce an output $\underline{u}(t)$ and $\underline{u}(t)$ drives a laser modeled as a voltage controlled oscillator centered at f_0, the pdf of the laser output frequency is the same as the pdf of $\underline{u}(t)$, i.e., gaussian. A nonlinear plant would be required in order to accurately model a homogeneously broadened laser line, which is Lorentzian, since only through a nonlinear transformation can a gaussian process $\underline{u}_f(t)$ be transformed into a nongaussian process $\underline{u}(t)$. A Lorentzian random variable is also known as a Cauchy random variable. The pdf of a Cauchy distributed random variable is given by (Ref.19:48):

$$f_x(x) = \frac{1}{\pi} \cdot \frac{a}{a^2+(x-m_x)^2} \tag{94}$$

(Technically, of course, none of the moments of this density exist. That is, $\int x^n f_x(x)dx$ does not converge over infinite limits for $n>0$). Of course, an approximation would still be made later, when the estimator equations are linearized in a Taylor series expansion and this will result in a different modeling error.

V. Simulation of Kalman Filter Processor

In this chapter the signal models of chapter IV are simulated and the results of the simulations are discussed. Comparisons are made with CR bounds and a linearized first order PLL. Some interesting behavior on the part of the processor is noted and explained.

Simulation Parameters

A subroutine was written in Fortran IV which performs a Monte Carlo simulation of the processor of interest. The simulator performs an ensemble average over a user determined number of realizations of the measurement noise process. The subroutine is listed in Appendix C.

For the case where the IF is fixed and known (no doppler shift is present), the phase was modelled in one dimension and two models were investigated. The first model was for the phase a constant. The second model was for the phase executing a random walk around the unit circle. These two models were chosen because they represent two extremes in the degree of correlation of the phase process and are typically the models encountered in the literature (Ref.13:939, Ref.8:48). Neither the constant phase plant model nor the random walk phase plant model may be adequate for any particular case, but since they bracket the process

correlations likely to be encountered, they can serve as upper and lower bounds, respectively, on how well the filter will perform in practice.

Also simulated was the case where the phase is executing a random walk and there is a constant, unknown, doppler shift. The errors in jointly estimating both phase and frequency are investigated.

In all simulations 100 sequential time estimates of the phase process are computed and each estimate is ensemble averaged over 100 realizations of the noise process. One hundred realizations of the noise is not very many, but it is common practice in Monte Carlo simulations to use a number of realizations that is relatively small compared to what the central limit theorem might deem prudent for a reasonable confidence in the statistics (Ref.16:939, 15:382, 10:67). Compared to the references cited, 100 is a rather large number of realizations. The reason that so few realizations are used is the quantity of computer time consumed. One run of the subroutine with 100 realizations and 100 recursions will consume about 10 to 15 seconds of CP time. For a 0.9 probability that the phase error estimate is within 0.1 radians of the actual phase error, the central limit theorem would require 809 realizations. The weak law of large numbers would require 3290 realizations (Ref.10:67). The Chernoff bound requires 1515 realizations (Ref.19:97).

Constant Phase Processor

For the constant phase processor, the phase was modelled as a random variable uniformly distributed between $-\pi$ and π radians. Initial values were then $\underline{\bar{x}}_0=\bar{\theta}_0=0$, $P_0=\pi^2/3$. P_0 is the variance of the a-priori estimate θ_0. The state vector is one-dimensional. A value of $P_t=4$ integrals per IF period T was used.

Figure 5 shows the simulation results for an actual angle of $\theta=0$ and three different CNR's of +30db, +10db, and -10db. For CNR=30db, the processor converges almost immediately to the correct value. For CNR=-10db, the processor fails to converge at all after 100 recursions. Because the derivation of the Kalman filter performed by Sage discarded all terms in a Taylor series expansion of $\underline{\hat{x}}_k$ and P_k beyond the first order, the estimator does not perform well in a high noise environment. In a high noise environment, the assumption of approximate linearity of the processor around a best a-priori estimate trajectory (the best estimate of $\underline{x}_{k+1}$ before measurement $\underline{r}_{k+1}$ is incorporated, $\underline{\hat{x}}^b_{k+1}=\phi\underline{\hat{x}}_k$) is violated and consequently the filter no longer adequately extracts information from the measurements. As a result, the processor fails to converge. In the low CNR environment, the processor variance does not settle to a steady state value as it does in the high CNR environment, but rather it oscillates about, never reaching a steady state. The processor simply tracks the noise.

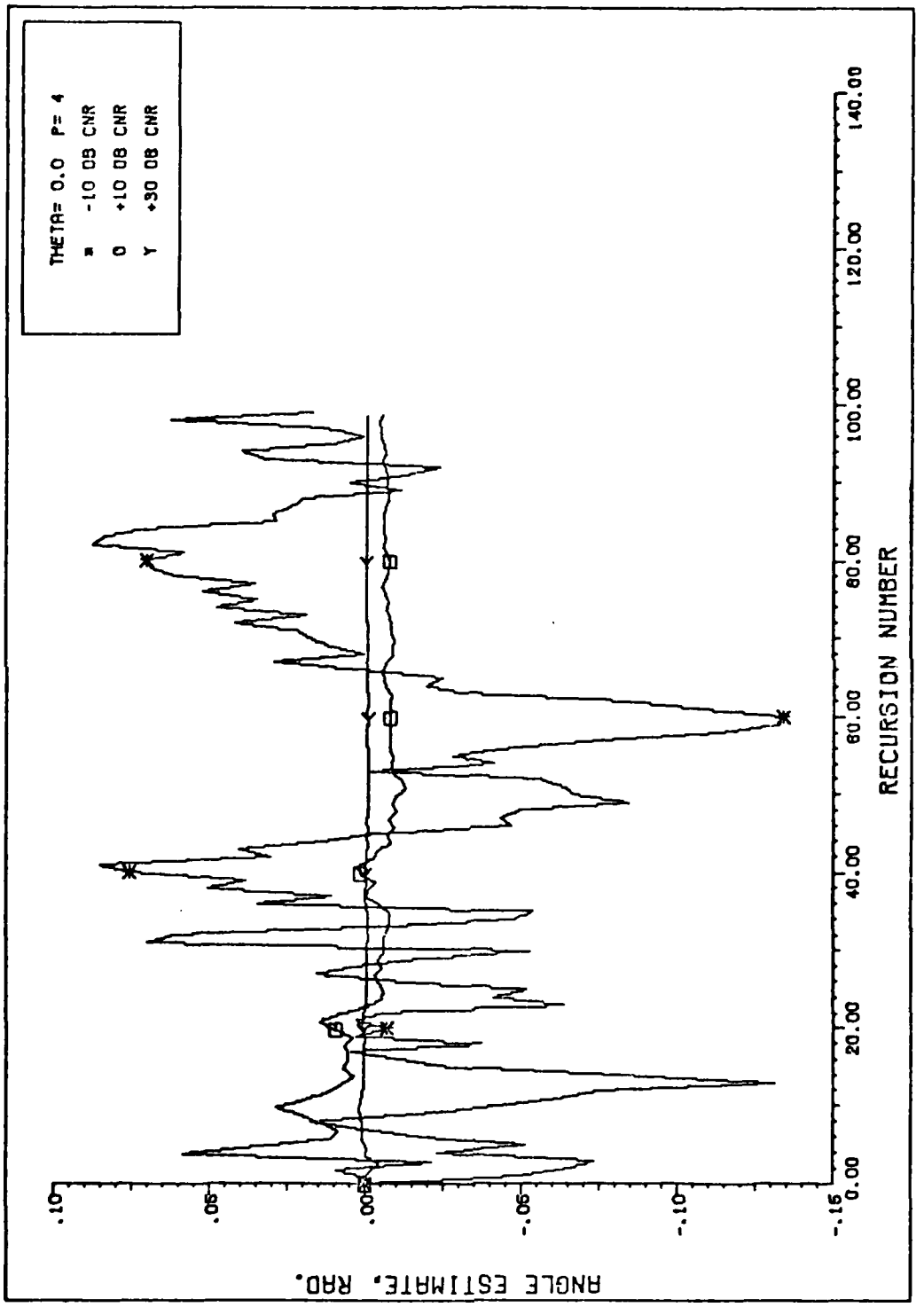

Figure 5. Constant Phase Processor Output

For CNR=10db, the processor does converge after about 25 recursions, but it converges to the wrong value, about $\hat{\theta}_{100}$=-0.01 radians (-0.57°). The processor is biased. Many texts either assume that nonlinear Kalman filters are unbiased or state without proof, justification or conditioning that the bias is zero (Ref.14:433). As discussed in Maybeck (Ref.8), these claims are false. Maybeck discusses methods for reducing the bias of the processor by using second order approximation filters (retaining Taylor series terms up to order 2), or by using first order filters (like this one) but adding bias correction terms taken from the second order filter equations. These methods result in somewhat more complicated filter algorithms and were not used in this research, however, processor biases will be pointed out as they are encountered.

To investigate the bias problem further, Figure 6 plots the estimation error after 100 recursions, $\hat{\theta}_{100}-\theta$, which should be very close to the actual bias, for three CNR's. First, notice that for CNR=-10 db, the bias varies linearly (approximately) with the actual angle θ. This is because the processor is tracking the noise which is zero mean and tends to guess $\theta=0$, the a-priori estimate, on the average. Also notice that even for a very high CNR, 30db, the processor guesses $\hat{\theta}=0$, on the average, whenever $\theta=\pm\pi/2$. This phenomenon is a direct result of the modulo-π ambiguity of

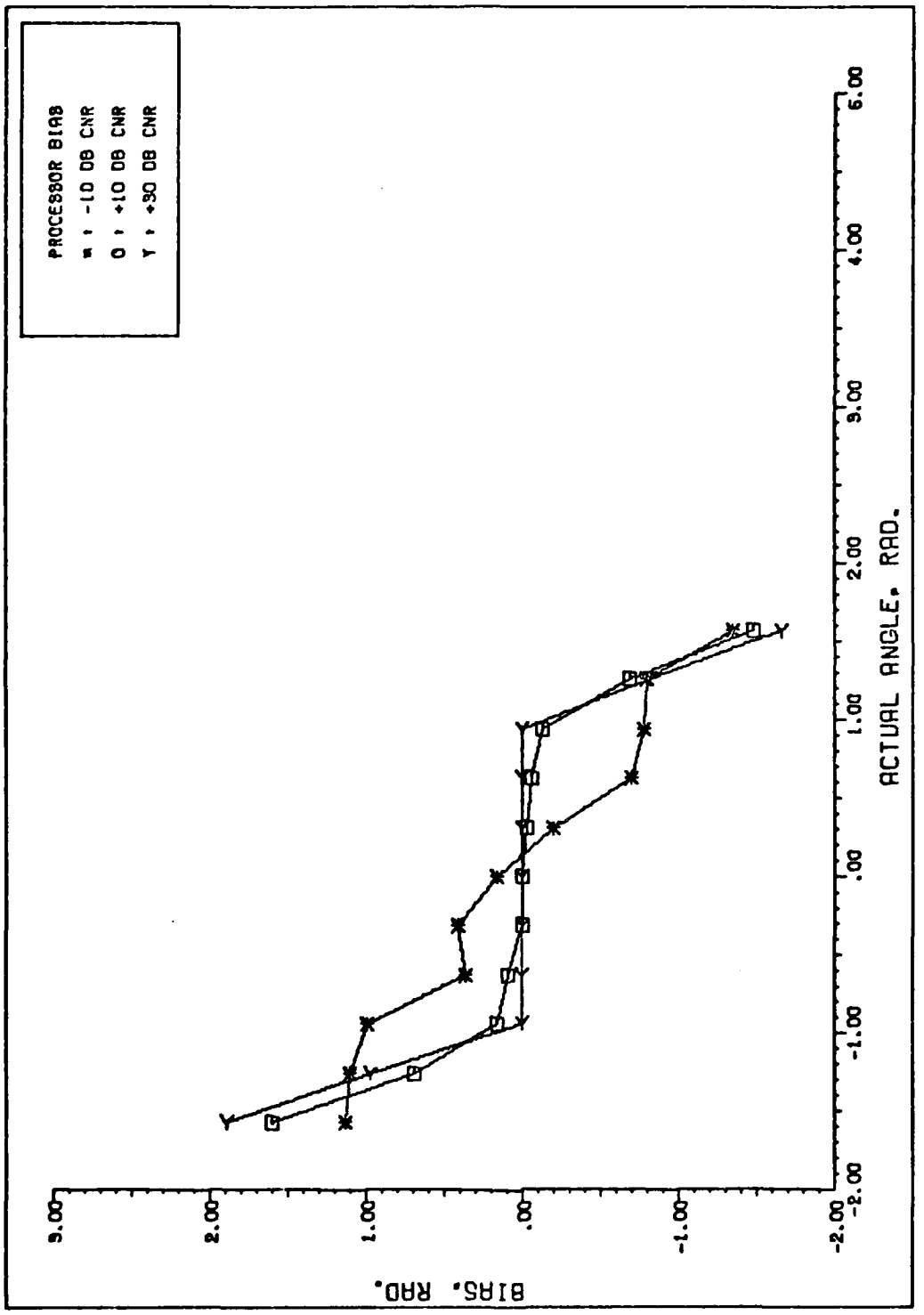

Figure 6. Constant Phase Processor Bias

the processor. If the actual angle is $+\pi/2$, the processor may determine an estimate that, due to noise corruption, is $\hat{\theta} \pm \varepsilon$, where $\varepsilon > 0$ is the error. But $\frac{\pi}{2} + \varepsilon$ (or $-\frac{\pi}{2} - \varepsilon$) is outside the ambiguity range of the processor and so it guesses $-\frac{\pi}{2} + \varepsilon$ (or $\frac{\pi}{2} - \varepsilon$). That is, the processor "wraps around" the semicircle and the average over many realizations is zero. This explains why, even though the estimate seems poor from the examination of a sample mean, the variance, P_k, still gets small as k gets large. It also explains why the bias rises, for CNR=10db, as $\theta \to \frac{\pi}{2}$. With the higher noise level, as the angle gets closer to $-\frac{\pi}{2}$, the processor will "wrap around" more often and the bias will rise. Similarly, for a fixed angle, the processor will "wrap around" more often for a smaller CNR, so the bias increases as CNR decreases.

Figure 7 is a plot of the inverse variance ($P_{100}^{-1} = \sigma_{\hat{\theta}_{100}}^{-2}$) versus the CNR. Also plotted is the theoretical CR bound and the variance for the linearized PLL. The processor significantly underperforms the PLL, although this gap would narrow if P_t was increased. The processor almost reaches its CR bound with equality, however. After 100 recursions, the estimator is "almost efficient".

Random Phase Walk

The next model simulated is for the phase executing a random walk around the unit circle. For this case, the variance of the walk, or diffusion, parameter was set at

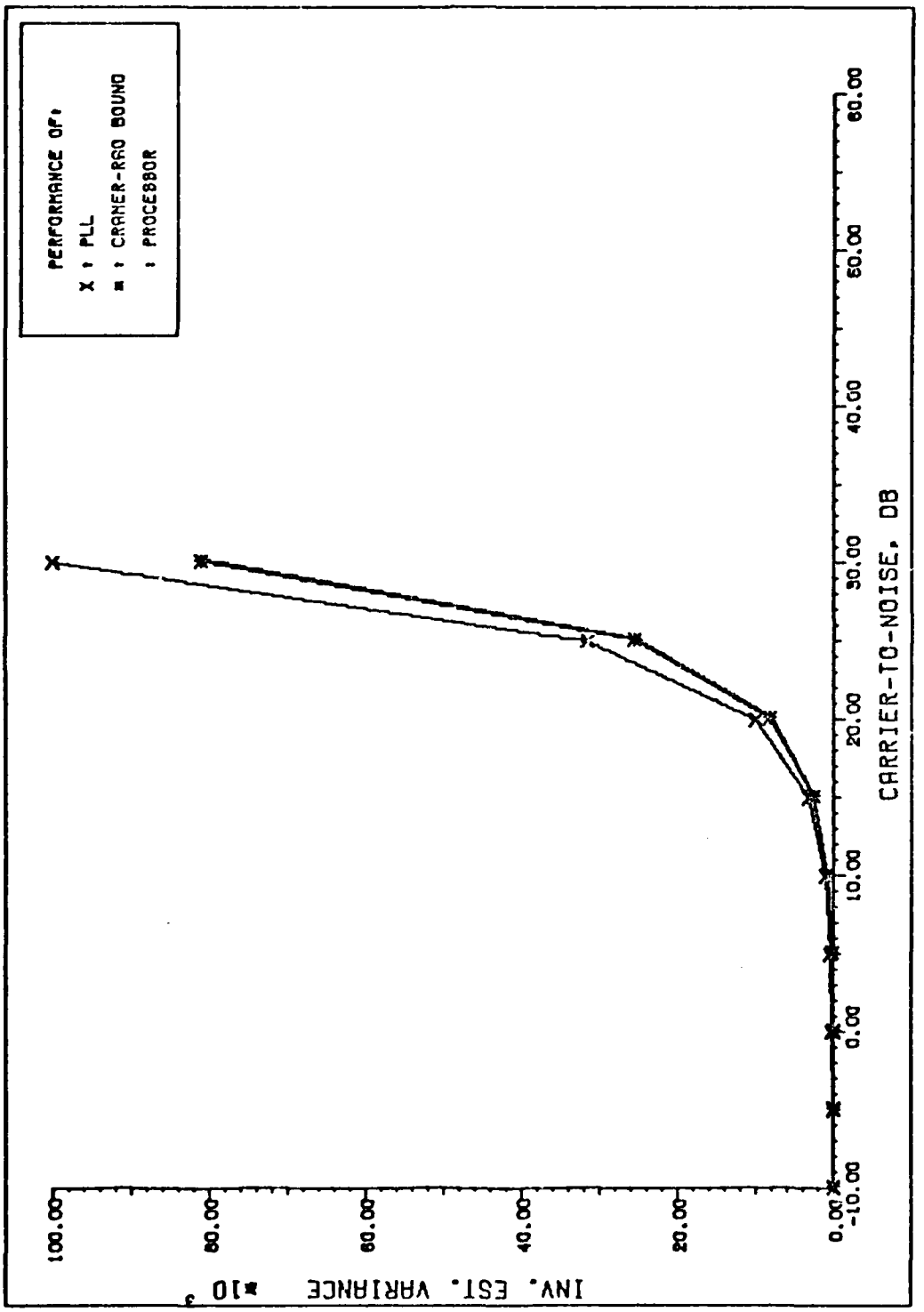

Figure 7. Constant Phase Processor Variances

$Q=0.005$ so that the size of the "steps" in the walk would be small enough that the phase can be assumed approximately constant over each IF period. For this value of Q, the magnitude of $\theta_{k+1}-\theta_k$ is less than 0.1 radians (5.7^0) with probability 0.84. Only one realization of the phase process was examined and the processor's performance was, again, averaged over 100 noise process realizations. Ideally, the processor's performance should be averaged over many realizations of the phase process as well as averaging over many realizations of the noise process. This averaging was not performed because of the amount of computer time that it would have consumed.

Figure 8 shows the error performance of the processor plotted for 100 recursions at 3 CNR's. The quantity plotted is the estimator error, $\hat{\theta}_k-\theta_k$. The reduction in performance at progressively lower CNR's is self evident. Note, however, that the processor, at 10db CNR, tends to made more negative errors than positive errors. This is another indication of the processor bias. The bias is even more evident for the CNR=-10db case. For this particular realization of the walk, the phase managed to walk as far as +1.4 radians, which is quite close to $+\frac{\pi}{2}$. For a walk realization which does not walk as far from $\theta=0$, the error, on the average, would be expected to be less. Simulations confirm that this is true, although the processor still makes

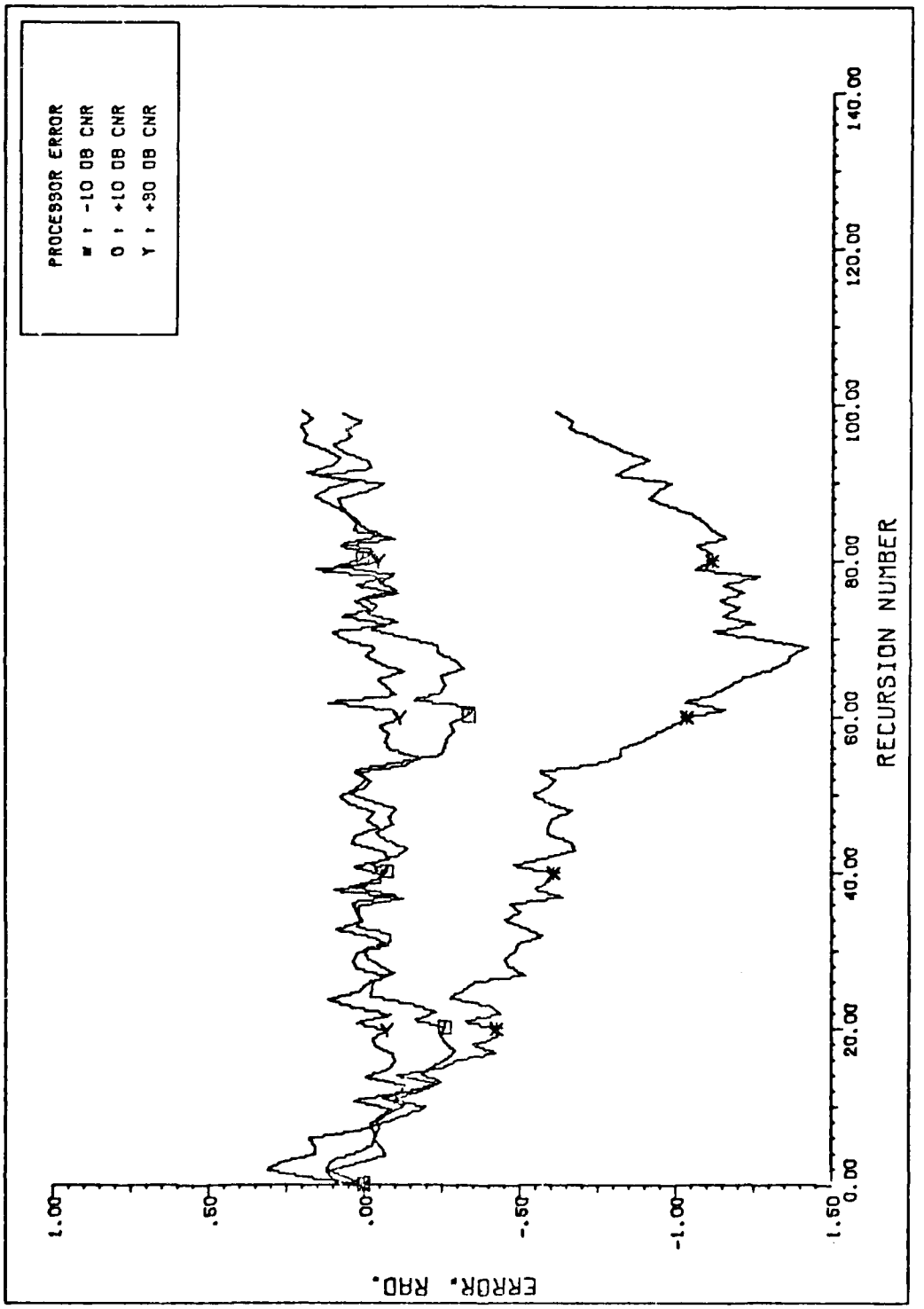

Figure 8. Random Walk Processor Output Error

significantly more errors for the lower CNR.

Figure 9 plots the inverse error variance versus the CNR along with the CR bound and the theoretical results for the linearized PLL. The scale on the vertical axis has been changed relative to Figure 7. This change reflects the increased bandwidth of the process and the corresponding increase in the bandwidth of the PLL loop filter. The loop filter time constant has gone from KT, where $K=k_{max}=100$, to T . The fact that the processor seems to outperform its CR bound can be explained on the basis of the fact that the computation of the CR bound in equation (24) set $K=1$. That is, the CR bound is for a processor which does not take into account the a-priori information on the correlation of the phase process. The processor simulated here does use this a-priori information and it gives a lower variance estimate as a result.

Since the processor is biased, and the CR bound was derived for an unbiased estimator, it might be argued that the processor outperforms its CR bound because the bound was derived for the unbiased case. The CR bound for a biased estimator is given by multiplying the right hand side of equation (11), (the bound for an unbiased estimator) by $(1-db(\theta)/d\theta)^2$, where $b(\theta)$ is the processor bias as a function of θ (Ref.17:146). From Figure 6, for moderate to high CNR's, $db(\theta)/d\theta \approx 0$ for all angles not close to $\pm\frac{\pi}{2}$.

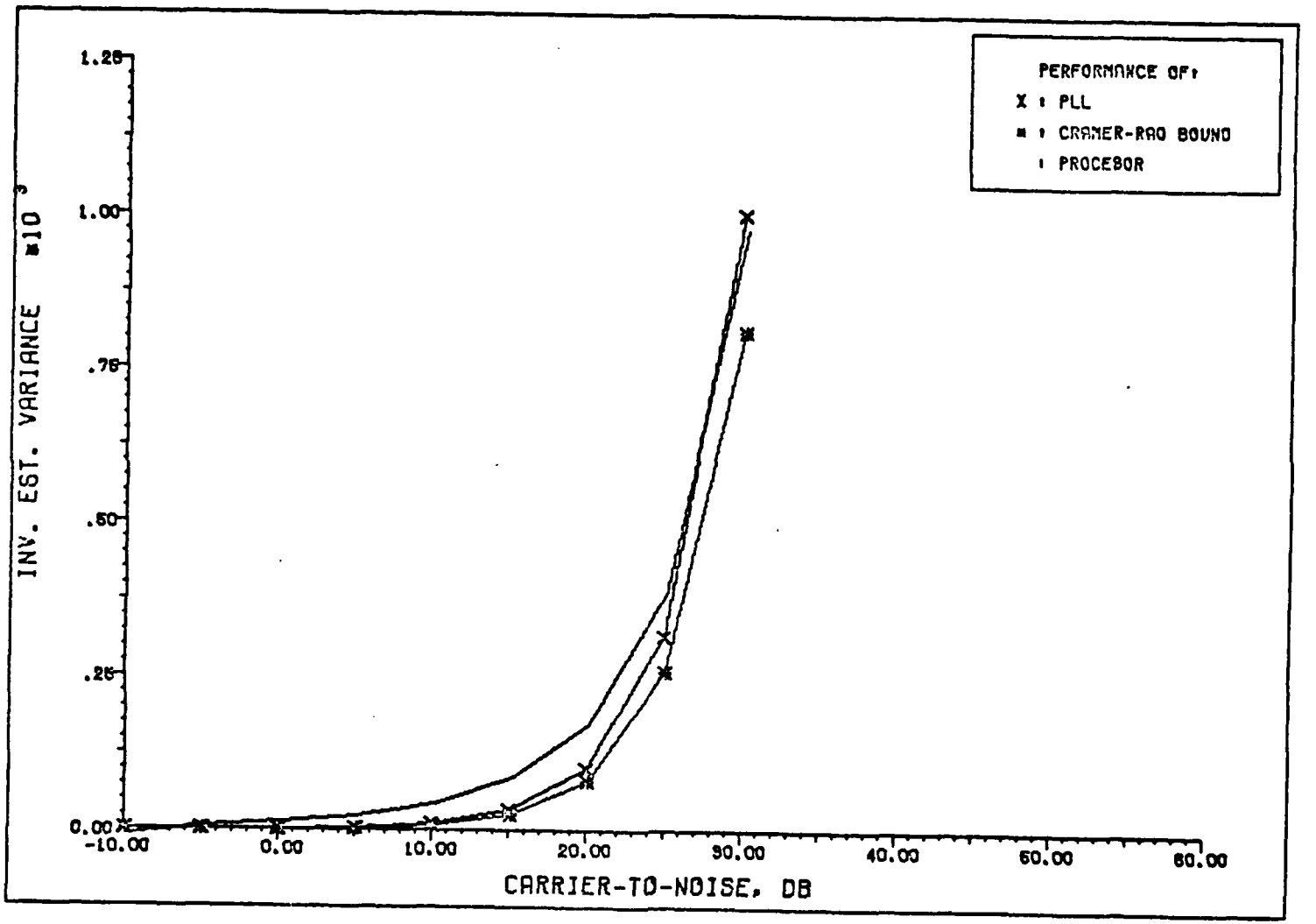

Figure 9. Random Walk Processor Variances

At low CNR's, the Kalman filter also outperforms the PLL. This is also due to the fact that the PLL does not incorporate a-priori information about the plant dynamics, whereas the Kalman filter does incorporate this information.

Phase Estimation with Doppler Shift

It was mentioned earlier that phase and frequency can be estimated jointly. The state vector becomes two dimensional with components x_1=doppler shift and x_2=phase. The phase process was modelled as a random walk with diffusion parameter $Q=0.005$. A static model of the doppler shift was assumed with a shift of +2MHz. The IF was chosen at $1/T=50$MHz. If the filter is in a 1.06μ Nd:YAG laser receiver, this corresponds to a relative target velocity of about 5 mph (2.1 mtrs/sec), a rather small velocity and doppler shift. The following model parameters were used for the simulation:

$$Q = \begin{bmatrix} 0 & 0 \\ 0 & 0.005 \end{bmatrix} \quad \phi = \begin{bmatrix} 1 & 0 \\ T & 1 \end{bmatrix} \quad P_0 = \begin{bmatrix} 3.6\text{x}10^{13} & 1.09\text{x}10^{6} \\ 1.09\text{x}10^{6} & \pi^2/3 \end{bmatrix}$$

$$\underline{x}_0 = \begin{bmatrix} 0 \\ 0 \end{bmatrix} \quad P_t = 4 \qquad (95)$$

One hundred recursive estimates were simulated and averaged over 20 realizations of the measurement noise.

The P_0 matrix was chosen iteratively in an effort to get the filter to converge without tracking the noise (Ref. 7:338). Initially, P_{011} was set to 36 THz^2 by assuming that the frequency error or doppler is normally distributed with standard deviation 6 MHz. The phase variance, P_{022}, was again chosen at $\pi^2/3$. The initial trial of $P_{012}=P_{021}$ was $\sqrt{P_{011}P_{022}}=1.09\times10^7$ but this value was too large and caused the estimator to track the measurement noise. Examination of the estimator equation (57) indicates that the element P_{k12} influences the update of x_1, so P_{012} was reduced until the filter converged more quickly to the actual variance of its estimates (or something close to it in this case).

At 30 and 10db CNR, the filter makes the following average errors and standard deviations:

$$\text{CNR=30 db:}\quad \underline{\hat{x}}_{20}-\underline{x} = \begin{bmatrix} .56\text{MHz} \\ -.024\text{rad} \end{bmatrix} \begin{matrix} (\sigma_{20})_{11} = .357\text{MHz} \\ (\sigma_{20})_{22} = .102\text{rad} \end{matrix} \tag{96}$$

$$\text{CNR=10 db:}\quad \underline{\hat{x}}_{20}-\underline{x} = \begin{bmatrix} .39\text{MHz} \\ -.10\text{rad} \end{bmatrix} \begin{matrix} (\sigma_{20})_{11} = .375\text{MHz} \\ (\sigma_{20})_{22} = .159\text{rad} \end{matrix} \tag{97}$$

The processor exhibits little degradation in performance

when the CNR drops from 30db to 10db compared to a similar drop when the frequency is known exactly. However, the variances of the errors are significantly higher than the error variances for the same CNR's when the frequency is known exactly. No comparisons were made with other processors, but the phase estimate seems better than might intuitively be expected for the given error in the estimate of the frequency error ($\sim$30%). This is not that surprising since the actual frequency is 52MHz, an error in the estimate of the offset of 500KHz gives a fractional frequency error of less than 1%.

VI. Conclusions and Recommendations

A nonlinear Kalman filter has been derived to estimate the phase of a carrier measured through an IDF. Two models of the phase process were examined and one case involving doppler shift was also examined, though not in depth. The problem was motivated by an optical heterodyne receiver structure, but the solution formulation was much more general in nature. Any system which processes samples like those in equation (25) could use all or part of the theoretical development in this thesis.

Conclusions

This study has demonstrated that it is possible to estimate the phase of an optical field with detectors which are much lower in bandwidth than the heterodyned waveform at the IF. The only requirement placed on the system is that the integration time of the detector be small enough that the phase and amplitude can be treated as constants over the integration period.

Although the processor shows no significant improvement over the linearized PLL for the two phase models examined, the PLL could be utilized only in conjunction with wideband detectors. Thus, this system allows phase measurements where they would otherwise be impossible. Also, for

cases where distributed phase measurements are desirable, wideband detectors are generally not available in large arrays, but CCD's are.

The few simulations performed have also indicated that it is possible to estimate relative frequency, doppler or LO instabilities, in addition to relative phase. These simulations have also indicated that the phase can be tracked even with a relatively poor estimate of the frequency available. The system is not too sensitive to the actual LO frequency.

Recommendations

The measurement equation (25) was derived on the basis of two simplifying assumptions: the amplitude and the phase are both approximately constant over the measurement interval. Since a CCD inherently averages over a rather long period of time compared to T, the first assumption would probably be violated in a rapidly fading environment or where the carrier has incidental AM of wide bandwidth compared to the integration time. Similarly, the second assumption could be investigated by allowing the phase to drift during the measurement interval.

The presence of a modulo-π ambiguity in the processor is a drawback, but it might be possible to eliminate it. One possible method to accomplish this was suggested by Meer (Ref.10:106). That method consists of checking to see

if $\hat{\theta}_k$ is close to $\pm \frac{\pi}{2}$. If it is, and $\hat{\theta}_{k+1}$ is also close to $\pm \frac{\pi}{2}$ and has sign opposite that of $\hat{\theta}_k$, then a new estimate of θ_{k+1} can be defined:

$$\hat{\theta}'_{k+1} = \hat{\theta}_{k+1} \pm \pi \tag{98}$$

The sign in front of the π depends on whether $\hat{\theta}_k$ was positive or negative. In the absence of noise, this procedure could regenerate the phase sequence with no ambiguity. In the presence of noise, the number of errors committed would depend on how small the parameter $\delta = \frac{\pi}{2} - |\hat{\theta}_k|$ is permitted to become and how small $\delta' = \frac{\pi}{2} - |\theta_{k+1}|$ must also become before a correction is made, provided $\hat{\theta}$ changes sign. Clearly, more errors would also be made as the CNR is decreased.

This procedure is somewhat ad-hoc. A more mathematically precise method would be to take advantage of both the in phase and quadrature information contained in the measurement. The update portion of the covariance matrix, the term $\beta\cos(\theta_{k+1} - \hat{\theta}'_k) + n_{kc}$ in equation (66), or the algebraically equivalent part of equation (58), is the part that incorporated new measurement information into the covariance equation. If $|\theta_{k+1} - \hat{\theta}'_k| > \pi$, then a wrap around will occur and the update portion of the variance equation will be negative, since $\cos(x) < 0$ when $\pi < |x| < 2\pi$. Adding π to $\hat{\theta}_{k+1}$ if it falls into the fourth quadrant (or subtracting π from

$\hat{\theta}_{k+1}$ if it falls into the first quadrant) when the update term is negative will regenerate the phase sequence. If the noise variance becomes too large, clearly errors may be made, but the estimator does not perform well in very low CNR environments, anyway.

Much work remains open on the problem of estimating a multi-parameter state vector. In particular, the most interesting case from an optical communication point of view is the unstable LO tracking a random phase walk. The filter equations were derived in (92) and (93) (implicitly, at least), but performance simulations were only begun with a small, fixed unknown frequency shift. Extensions of this work would have practical applications to any laboratory or field system since LO instabilities are always present.

Since the main advantage of CCD detectors is their availability in large arrays which allow spatially distributed measurements, it would be logical to incorporate spatial information into the processor. If the phase of the received waveform or the background noise has a known or assumed correlation, then the entire array of measurements can be utilized to estimate the phase at each pixel. The incorporation of more a-priori information should result in a lower variance processor. Because of the conceivably large size of the array, either a piecewise correlation over small parts of the array would be assumed, or the array

could be processed in a spatially recursive fashion. The second alternative is especially intriguing since the question of the permissibility of recursive processing in two dimensions is not quite closed (Ref.11:935).

Bibliography

1. Csaki, Frigyes. Modern Control Theories. Budapest: Akademiai Kiado,1972.

2. CCD 211 Image Sensor Specification Sheet. Mountainview: Fairchaild Semiconductors, 1976.

3. Davenport, Wilbur B. and William L. Root. An Introduction to the Theory of Random Signals and Noise. New York: McGraw Hill, Inc.,1958.

4. Frantz, Lee M., Alexander A. Sawchuk, and Werner von der Ohe. "Optical Phase Measurement in Real Time," Applied Optics, 18:3301(1October 1979).

5. Gagliardi, Robert M. and Sherman Karp. Optical Communications. New York: John Wiley and Sons, 1976.

6. Gupta, Someshwar C. and Lawrence Hasdorff. Fundamentals of Automatic Control. New York: John Wiley and Sons,1970.

7. Maybeck, Peter S. Stochastic Models, Estimation and Control, Vol.1. New York: Academic Press, 1979.

8. -----. Stochastic Models, Estimation and Control, Vol.2. To be published.

9. McBride, Alan L., "On Optimum Sampled-Data FM Demodulation," IEEE Transactions on Automatic Control, AC-17:439(Aug.1972).

10. Meer, David E. Phase Sequence Estimation for Laser Line-Scan Imagery in the-Presence of Rayleigh Fading. Wright-Patterson AFB: AFIT MSEE Thesis,1979.

11. Mersereau, Russell M. "The Processing of Hexagonally Sampled Two Dimensional Signals," Proceedings of the IEEE,67: 930(June,1979).

12. Robinson, Stanley R. Optical Communications lectures and private communications, September 1979 to June 1980.

13. Sage, Andrew P. Optimum Systems Control. Englewood Cliffs: Prentice Hall, Inc.,1969.

14. Sage, Andrew P., and James L. Melsa. Estimation Theory with Applications to Communications and Control. New York: McGraw Hill Book Co.,1971.

15. Schweppe, Fred C. Uncertain Dynamic Systems. New Jersey: Prentice-Hall,1973.

16. Tam, Peter K.S., and John B. Moore. "A Gaussian Sum Approach to Phase and Frequency Estimation," IEEE Transactions on Communications, COM-25: 935(September 1977).

17. Van Trees, Harry L. Detection, Estimation, and Modulation Theory, Part I. New York: John Wiley and Sons,1968.

18. Viterbi, Andrew J. Principles of Coherent Communication. New York:McGraw-Hill Book Co.,1966.

19. Wozencraft, John M. and Irwin M. Jacobs. Principles of Communication Engineering. New York: John Wiley and Sons, Inc.,1965.

20. Wyant, J.C., "Use of an AC Heterodyne Lateral Shear Interferometer with Real-Time Wavefront Correction Systems," Applied Optics,14: 2622(November 1975),

Appendix A

Proof that Samples of a Sine Wave Sum to Zero

Numerous times in the text, a great deal of mathematical simplification resulted when terms of the form $\sin(\frac{2\pi}{P_t}(i-1)+\theta(t))$ and $\sin(\frac{4\pi}{P_t}(i-1)+\theta(t))$ summed from $i=1$ to $i=P_t$ were set to zero. Here this identity is established. Consider a slightly more general case where k is an arbitrary integer:

$$\sum_{i=1}^{P_t} \sin(\frac{2}{P_t}\cdot k\cdot(i-1)+\theta(t)) = \sum_{i=1}^{P_t} \sin(2\pi i\cdot\frac{k}{P_t} - \frac{2\pi k}{P_t} + \theta(t)) \tag{99}$$

Euler's identity states that $\exp(jx)=\cos(x)+j\sin(x)$, so, if it can be established that:

$$\sum_{i=1}^{P_t} \exp\left[j\{2\pi i\cdot\frac{k}{P_t} - \frac{2\pi k}{P_t} + \theta(t)\}\right] = 0 \tag{100}$$

then the proof is completed. The term $\exp\left[-j\cdot\frac{2\pi k}{P_t} + j\theta(t)\right]$ can be moved out of the summation since it does not depend on the index, i. Define a parameter $L=\exp(j2\pi k/P_t)$ so that a geometric series in L results. A geometric series sums as:

$$\sum_{i=1}^{P_t} L^i = \frac{L(1-L^{P_t})}{1-L} \tag{101}$$

Since k is an integer, $L^{P_t}=0$ unless $k=0$, so the sum in equation (100) is indeed zero for all $k\neq 0$, including the special cases of interest, $k=1$ and $k=2$.

Appendix B

Simplification of Estimator Equations

Several vector differentiation rules must be defined. The operator $\frac{\delta}{\delta \underline{x}^T}$ is a row vector which is always multiplied to the right of the vector on which it operates (Ref.1:983). For a 3-dimensional vector:

$$\frac{\delta \underline{f}(\underline{x})}{\delta \underline{x}^T} = \begin{bmatrix} f_1(\underline{x}) \\ f_2(\underline{x}) \\ f_3(\underline{x}) \end{bmatrix} \left[\frac{\delta}{\delta x_1} \quad \frac{\delta}{\delta x_2} \quad \frac{\delta}{\delta x_3} \right] \tag{102}$$

Similarly, the operator $\frac{\delta}{\delta \underline{x}}$ is a column vector which always operates to the left of a transposed column vector (Ref. 1:983):

$$\frac{\delta \underline{f}^T(\underline{x})}{\delta \underline{x}} = \begin{bmatrix} \frac{\delta}{\delta x_1} \\ \frac{\delta}{\delta x_2} \\ \frac{\delta}{\delta x_3} \end{bmatrix} \left[f_1(\underline{x}) \quad f_2(\underline{x}) \quad f_3(\underline{x}) \right] \tag{103}$$

Both differentiations result in matrices with elements like $\frac{\delta f_i(\underline{x})}{\delta x_j}$.

From the chain rules for these operators (Ref.1:985), the partial derivatives in equations (49) and (50) can be expanded:

$$\frac{\delta}{\delta \hat{\underline{x}}_k} \underline{h}^T(\underline{c}^T\phi\ \hat{\underline{x}}_k) = \frac{\delta(\underline{c}^T\phi\hat{\underline{x}}_k)^T}{\delta\hat{\underline{x}}_k} \cdot \frac{\delta\underline{h}^T(\hat{\theta}'_k)}{\delta\hat{\theta}'_k} \tag{104}$$

$$= \phi^T\underline{c}\ \frac{\delta\underline{h}^T(\hat{\theta}'_k)}{\delta\hat{\theta}'_k} \tag{105}$$

$$\frac{\delta}{\delta\hat{\underline{x}}_k^T} \underline{h}(\underline{c}^T\phi\hat{\underline{x}}_k) = \frac{\delta\underline{h}(\hat{\theta}'_k)}{\delta\hat{\theta}'_k} \cdot \underline{c}^T\phi \tag{106}$$

Equation (49) becomes:

$$\hat{\underline{x}}_{k+1} = \phi\hat{\underline{x}}_k + P_{k+1}\phi^{-T}\phi^T\underline{c}\ \frac{\delta\underline{h}^T(\hat{\theta}'_k)}{\delta\hat{\theta}'_k}\ R^{-1}\ \left[\underline{r}_{k+1} - \underline{h}(\underline{c}^T\phi\hat{\underline{x}}_k)\right] \tag{107}$$

$$\hat{\underline{x}}_{k+1} = \phi\hat{\underline{x}}_k + P_{k+1}\underline{c}\ \frac{\delta\underline{h}^T(\hat{\theta}'_k)}{\delta\hat{\theta}'_k}\ R^{-1}\ \left[\underline{r}_{k+1} - \underline{h}(\hat{\theta}'_k)\right] \tag{108}$$

which is equation (53). Equation (50) becomes:

$$P_{k+1} = P'_k\left[\phi^{-T} - \phi^{-T}\left\{\frac{\delta}{\delta\hat{\theta}'_k}\left[\phi^T\underline{c}\ \frac{\delta\underline{h}^T(\hat{\theta}'_k)}{\delta\hat{\theta}'_k}\ R^{-1}\left\{\underline{r}_{k+1} - \underline{h}(\hat{\theta}'_k)\right\}\right]\right\}\underline{c}^TP'_k\right]^{-1} \tag{109}$$

$$= P'_k\left[\phi^{-T} - \underline{c}\frac{\delta}{\delta\hat{\theta}'_k}\left[\frac{\delta\underline{h}^T(\hat{\theta}'_k)}{\delta\hat{\theta}'_k}\ R^{-1}\left\{\underline{r}_{k+1} - \underline{h}(\hat{\theta}'_k)\right\}\right]\underline{c}^TP'_k\right]^{-1} \tag{110}$$

The vector operators also obey the rule (Ref.1:985):

$$\frac{\delta}{\delta t}(A\underline{z}) = \frac{\delta A}{\delta t} \cdot \underline{z} + A \cdot \frac{\delta \underline{z}}{\delta t} \tag{111}$$

let $A=\dfrac{\delta \underline{h}^T(\hat{\theta}_k')}{\delta \hat{\theta}_k'}$ and let $\underline{z}=R^{-1}\{\underline{r}_{k+1}-\underline{h}(\hat{\theta}_k')\}$. Then:

$$P_{k+1} = P_k'\left[\phi^{-T}-\underline{c}\left\{\frac{\delta^2 \underline{h}^T(\hat{\theta}_k')}{\delta \hat{\theta}_k'^2} R^{-1}\left\{\underline{r}_{k+1}-\underline{h}(\hat{\theta}_k')\right\}\right.\right.$$

$$\left.\left. - \frac{\delta \underline{h}^T(\hat{\theta}_k')}{\delta \hat{\theta}_k'} \cdot R^{-1} \frac{\delta \underline{h}(\hat{\theta}_k')}{\delta \hat{\theta}_k'}\right\}\underline{c}^T P_k'\right]^{-1} \tag{112}$$

Which is equation (54).

Now substitute equations (25) through (27) into equations (53) and (54) along with $R=\sigma_n^2 I$, where I is a $P_t x P_t$ identity matrix. Write out the vector products as summations to give:

$$\hat{\underline{x}}_{k+1} = \phi\hat{\underline{x}}_k + P_{k+1}\,\underline{c} \cdot \frac{1}{\sigma_n^2} \sum - \frac{i_s^T\gamma}{\pi} \cdot \sin(\frac{\pi}{P_t})\sin(\frac{2\pi}{P_t}(i-1)+\hat{\theta}_k')$$

$$\cdot\left[r_{k+1}(i) - \frac{i_s^T\gamma}{\pi} \sin(\frac{\pi}{P_t})\cos(\frac{2\pi}{P_t}(i-1)+\hat{\theta}_k') - \frac{i_s^T}{P_t}\right] \tag{113}$$

Utilizing Appendix A and some trigonometric identities:

$$\hat{\underline{x}}_{k+1} = \phi\hat{\underline{x}}_k - \frac{i_s^T\gamma}{\pi\sigma_n^2}\cdot\sin(\frac{\pi}{P_t}) \sum r_{k+1}(i)\sin(\frac{2\pi}{P_t}(i-1)+\hat{\theta}_k')\cdot P_{k+1}\cdot\underline{c} \tag{114}$$

which is equation (57). Before doing similarly for equation (54), move the P_k' inside the inversion operation on the brackets:

$$P_{k+1} = \left[\phi^{-T}P_k'^{-1} - \underline{c}\left\{\frac{\delta^2 \underline{h}^T(\hat{\theta}_k')}{\delta\hat{\theta}_k'^2} R^{-1}\left\{\underline{r}_{k+1} - \underline{h}(\hat{\theta}_k')\right\} - \frac{\delta \underline{h}^T(\hat{\theta}_k')}{\delta\hat{\theta}_k'} R^{-1} \frac{\delta \underline{h}(\hat{\theta}_k')}{\delta\hat{\theta}_k'}\right\}\underline{c}^T\right]^{-1} \quad (115)$$

where the fact that $P_k'P_k'^{-1}=I$ was utilized. Now let $R^{-1}=1/\sigma_n^2 I$:

$$P_{k+1} = \left[\phi^{-T}P_k'^{-1} - \frac{1}{\sigma_n^2}\underline{c}\left\{\frac{\delta^2 \underline{h}^T(\theta_k')}{\delta\theta_k'^2}\left[\underline{r}_{k+1} - \underline{h}(\hat{\theta}_k')\right] - \left|\frac{\delta \underline{h}(\hat{\theta}_k')}{\delta\hat{\theta}_k'}\right|^2\right\}\underline{c}^T\right]^{-1} \quad (116)$$

Substituting for P_k' from equation (55) and utilizing (25)-(27):

$$P_{k+1} = \left[(\phi P_k \phi^T + GQG^T)^{-1} - \underline{c}\,\underline{c}^T \frac{1}{\sigma_n^2}\left\{-\frac{i_s^T\gamma}{\pi}\cdot\sin(\frac{\pi}{P_t})\cdot\cos(\frac{2\pi}{P_t}(i-1)+\hat{\theta}_k')\left[r_{k+1}(i) - \frac{i_s^T\gamma}{\pi}\sin(\frac{\pi}{P_t})\cos(\frac{2\pi}{P_t}(i-1)+\hat{\theta}_k') - \frac{i_s^T}{P_t}\right] - \sum(\frac{i_s^T\gamma}{\pi})^2\sin^2(\frac{\pi}{P_t})\sin^2(\frac{2\pi}{P_t}(i-1)+\hat{\theta}_k')\right\}\right]^{-1} \quad (117)$$

$$= \left[(\phi P_k \phi^T + GQG^T)^{-1} + \underline{c}\,\underline{c}^T \frac{1}{\sigma_n^2} \left\{ \frac{i_s T\gamma}{\pi} \cdot \sin(\frac{\pi}{P_t}) \sum r_{k+1}(i) \right.\right.$$

$$\cdot \cos(\frac{2\pi}{P_t}(i-1)+\hat{\theta}_k') - (\frac{i_s T\gamma}{\pi})^2 \sin^2(\frac{\pi}{P_t}) \cdot \sum \left[\cos^2(\frac{2\pi}{P_t}(i-1) \right.$$

$$\left.\left.\left. +\hat{\theta}_k') - \sin^2(\frac{2\pi}{P_t}(i-1)+\hat{\theta}_k') \right] \right\} \right]^{-1} \qquad (118)$$

$$= \left[(\phi P_k \phi^T + GQG^T)^{-1} + \underline{c}\,\underline{c}^T \frac{i_s T\gamma}{\pi\sigma_n^2} \cdot \sin(\frac{\pi}{P_t}) \sum r_{k+1}(i) \right.$$

$$\left. \cdot \cos(\frac{2\pi}{P_t}(i-1)+\hat{\theta}_k') \right]^{-1} \qquad (119)$$

which is just equation (58). Appendix A was used to eliminate the sum over the difference of two trigonometric terms squared in equation (118).

Now utilize the fact that, from equation (25):

$$r_k(i) = h_k(i)+n_k(i) \qquad (120)$$

$$= i_s T\left[\frac{1}{P_t} + \frac{\gamma}{\pi} \sin(\frac{\pi}{P_t})\cos(\frac{2\pi}{P_t}(i-1)+\theta_k)\right]+n_k(i) \qquad (121)$$

$$= \frac{i_s T}{P_t} + T\left[\frac{i_s \gamma}{\pi} \sin(\frac{\pi}{P_t})\cos(\frac{2\pi}{P_t}(i-1)+\theta_k)+\frac{1}{T} n_k(i)\right] \qquad (122)$$

$$= \frac{i_s T}{P_t} + T\, z_k(i) \qquad (123)$$

The $z_k(i)$ defined in equation (63) appears naturally. Now substitute this into equation (114), use Appendix A, and multiply by $(\frac{i_s^{\gamma}}{\pi})(\frac{\pi}{i_s^{\gamma}})=1$.

$$\underline{\hat{x}}_{k+1} = \phi\underline{\hat{x}}_k - \frac{i_s^{T\gamma}}{\pi\sigma_n^2}\sin(\frac{\pi}{P_t})(\frac{i_s^{\gamma}}{\pi})(\frac{\pi}{i_s^{\gamma}})T\sum z_{k+1}(i)$$

$$\cdot\sin(\frac{2\pi}{P_t}(i-1)+\hat{\theta}_k') \qquad (124)$$

$$= \phi\underline{\hat{x}}_k - (\frac{i_s^{T\gamma}}{\pi})^2\cdot\frac{1}{\sigma_n^2}\cdot\sin(\frac{\pi}{P_t})\cdot\frac{\pi}{i_s^{\gamma}}\sum z_{k+1}(i)$$

$$\cdot\sin(\frac{2\pi}{P_t}(i-1)+\hat{\theta}_k') \qquad (125)$$

$$= \phi\underline{\hat{x}}_k - \frac{1}{\pi^2}(\frac{\pi}{i_s^{\gamma}})\cdot 2\cdot\left[\frac{(i_s^{\gamma})^2}{2}\cdot\frac{T^2}{\sigma_n^2}\right]\cdot\sin(\frac{\pi}{P_t})$$

$$\cdot\sum z_{k+1}(i)\sin(\frac{2\pi}{P_t}(i-1)+\hat{\theta}_k') \qquad (126)$$

$$= \phi\underline{\hat{x}}_k - \frac{2P_t}{i_s^{\gamma}\pi}\cdot\mathrm{CNR}\cdot\sin(\frac{\pi}{P_t})\sum z_{k+1}(i)\sin(\frac{2\pi}{P_t}(i-1)+\hat{\theta}_k') \qquad (127)$$

The factor CNR was defined in (62) and can be verified by substituting equation (15) for σ_n^2 and remembering that:

$$n_k'(i) = \frac{1}{T}\,n_k(i) \rightarrow \sigma_n^{2\prime} = \frac{1}{T^2}\,\sigma_n^2 \qquad (128)$$

In equation (60) the factor $\frac{\sqrt{2}}{\pi}$ appears instead of $\frac{2}{i_s^{\gamma}\pi}$ because it is assumed throughout the paper that the signal power is normalized, $\frac{1}{2}(i_s^{\gamma})^2=1$, and fluctuations in the CNR are modelled only as fluctuations in σ_n^2 , $\sigma_{n'}^2$, or N_0 . The exact same arguments for equation (58) would lead to equation (61).

Now examine the term in equation (127):

$$\sum z_{k+1}(i)\sin(\frac{2\pi}{P_t}(i-1)+\hat{\theta}_k') = \sum\left[\frac{i_s^{\gamma}}{\pi}\sin(\frac{\pi}{P_t})\cos(\frac{2\pi}{P_t}(i-1)+\theta_{k+1})\right.$$

$$\left.\cdot\sin(\frac{2\pi}{P_t}(i-1)+\hat{\theta}_k')+n_{k+1}'(i)\sin(\frac{2\pi}{P_t}(i-1)+\hat{\theta}_k')\right] \qquad (129)$$

$$= \sum\frac{i_s^{\gamma}}{2\pi}\sin(\frac{\pi}{P_t})\sin(\hat{\theta}_k'-\theta_{k+1})+n_{k+1}'(i)\sin(\frac{2\pi}{P_t}(i-1)+\hat{\theta}_k') \qquad (130)$$

$$= -\frac{i_s^{\gamma}P_t}{2}\sin(\frac{\pi}{P_t})\sin(\theta_{k+1}-\hat{\theta}_k') + n_{ks} \qquad (131)$$

Similarly for equation (118):

$$\sum z_{k+1}(i)\cos(\frac{2\pi}{P_t}(i-1)+\hat{\theta}_k') = \frac{i_s^{\gamma}P_t}{2\pi}\sin(\frac{\pi}{P_t})\cos(\theta_{k+1}-\hat{\theta}_k)+n_{kc} \qquad (132)$$

where n_{kc} is defined in an obvious manner. Since n_{ks} and n_{kc} are both the sums of weighted gaussian variables, they are also gaussian, so it suffices to compute their second moments.

$$E\left[n_{ks}\right] = E\left[\sum n'_{k+1}(i)\sin\left(\frac{2\pi}{P_t}(i-1)+\hat{\theta}'_k\right)\right] \tag{133}$$

$$= \sum E\left[n'_{k+1}(i)\ \sin\ \left(\frac{2\pi}{P_t}(i-1)+\hat{\theta}'_k\right)\right] \tag{134}$$

$$= \sum E_{\hat{\theta}}\left[E_{n|\hat{\theta}}\left[n'_{k+1}(i)\sin\left(\frac{2\pi}{P_t}(i-1)+\hat{\theta}'_k\right)\right]\right] \tag{135}$$

$$= \sum E_{\hat{\theta}}\left[E_n\left[n'_{k+1}(i)\right]\sin\left(\frac{2\pi}{P_t}(i-1)+\hat{\theta}'_k\right)\right] \tag{136}$$

$$= 0 \tag{137}$$

Where the identity $E_{xy}\left[x(y)\right]=E_y\left[E_{x|y}\left[x|y\right]\right]$ was used, as was the fact that $n'_k(i)$ is zero mean. It is easily shown that $E\left[n_{kc}\right]=0$. Since n_{kc} and n_{ks} are zero mean, their variances are their second moments.

$$E\left[n_{ks}n_{k's}\right] = E\left[\sum_i\sum_j n'_i(k+1)\ n'_k(k\neq 1)\sin\left(\frac{2\pi}{P_t}(i-1)+\hat{\theta}'_k\right)\right.$$
$$\left.\cdot\sin\left(\frac{2\pi}{P_t}(j-1)+\hat{\theta}'_{k'}\right)\right] \tag{138}$$

$$= E_{\hat{\theta}}\left[\sum_i\sum_j E_n\left[n_i'(k+1)n_j'(k'+1)\right]\cdot\tfrac{1}{2}\cdot\{\cos(\tfrac{2\pi}{P_t}(i-1)\right.$$

$$\left.+\hat{\theta}_k-\hat{\theta}_{k'}')-\cos(\tfrac{2\pi}{P_t}(i+j-2)+\hat{\theta}_k'+\hat{\theta}_{k'}')\}\right] \qquad (139)$$

$$= E_{\hat{\theta}}\left[\sum_i E_n\left[n_i'(k+1)n_i'(k'+1)\right]\cdot\tfrac{1}{2}\right] \qquad (140)$$

$$= \frac{P_t}{2}\cdot\sigma_{n'}^2\ \delta_{kk'} \qquad (141)$$

The fact that $E_n\left[n_i'(k+1)n_j'(k'+1)\right]=\sigma_{n'}^2\delta_{kk'}$ was used since n_i' is white. Similarly,

$$E\left[n_{kc}n_{k'c}\right] = \frac{P_t}{2}\ \sigma_{n'}^2\delta_{kk'} \qquad (142)$$

$$E\left[n_{kc}n_{k's}\right] = 0 \qquad (143)$$

So, $\{n_{kc}\}$ and $\{n_{ks}\}$ are spectrally white sequences, mutually independent, and gaussian.

The above derivations, plus letting $(i_s\gamma)^2/2=1$, result in equations (65) and (66).

Appendix C

Simulation Subroutine

```
      SUBROUTINE GENSIM(Y,P,YO,PO,YACT,Q,PHI,KMAX,ITER,
     *IYDIM,IPT,CNRDB,SUMP,SUMY,N,KMPT,WKAREA)
      DOUBLE DSEED
      REAL N
      DIMENSION Y(IYDIM,KMAX),P(IYDIM,IYDIM,KMAX),YO(IYDIM)
      DIMENSION PO(IYDIM,IYDIM),Q(IYDIM,IYDIM)
      DIMENSION YACT(IYDIM,KMAX),PHI(IYDIM,IYDIM)
      DIMENSION SUMY(IYDIM,KMAX),SUMP(IYDIM,IYDIM,KMAX)
      DIMENSION WKAREA(KMPT),N(KMPT)
C
C*************************************************************
C
C  2D LT MARTIN B. MARK, GEO-80D, 22 SEP 80
C
C  THIS SUBROUTINE IS A GENERALIZED SIMULATOR FOR THE DE-
C  MODULATION OF A SIGNAL ENCODED ON THE PHASE OF A SINE-
C  WAVE.  VIRTUALLY ANY PHASE PLANT MODEL CAN BE ACCOMO-
C  DATED.  INTEGRATED SAMPLES OF THE RECEIVED WAVEFORM
C  ARE GENERATED AND USED IN AN EXTENDED KALMAN FILTER
C  TO DEMODULATE THE SIGNAL.
C  THE VARIABLES USED HAVE THE FOLLOWING SIGNIFICANCES:
C
C     Y(I,K)           K-TH STATE VECTOR ESTIMATE
C     P(I,J,K)         K-TH VARIANCE MATRIX
C     YO(I)            INITIAL STATE VECTOR
C     PO(I,J)          INITIAL VARIANCE MATRIX
C     YACT(I,K)        ACTUAL STATE VECTOR SEQUENCE
C     Q(I,J)           PLANT NOISE VARIANCE MATRIX
C     PHI(I,J)         PLANT TRANSITION MATRIX
C     KMAX             NUMBER OF SEQUENTIAL ESTIMATES OF Y
C     ITER             NUMBER OF ITERATIONS Y IS AVERAGED
C                      OVER
C     IYDIM            DIMENSIONALITY OF STATE VECTOR
C     IPT              SAMPLES OF INPUT WAVEFORM PER
C                      PERIOD
C     CNRDB            CARRIER-TO-NOISE RATIO, DB
C     KMPT             NUMBER OF NOISE SAMPLES TO BE GEN-
C                      ERATED BY GGNML
C     SUMP,SUMY,
C     N,WKAREA         SCRATCHPAD MATRICES
C
C  IMSL LIBRARY ROUTINES GGNML AND LINV3F ARE USED TO
C  GENERATE GAUSSIAN NOISE SAMPLES AND INVERT A MATRIX,
C  RESPECTIVELY.  SUBROUTINES NEWP, NEWY, AND SUMM ARE
C  ALSO UTILIZED AND ARE ATTACHED AT THE END OF GENSIM.
C  THE PHASE ANGLE IS ALWAYS THE LAST ELEMENT OF THE
C  STATE VECTOR Y.  ALL OTHER ELEMENTS OF THE STATE VEC-
C  TOR ARE ALSO COMPUTED AND RETURNED, BUT THEIR PHY-
C  SICAL SIGNIFICANCES ARE ARBITRARY.
C
C*************************************************************
C
C  INITIALIZE CONSTANTS
C
```

```
      KWD=2*IYDIM
      PI=3.141592654
      PT=FLOAT(IPT)
      CNR=10.**(CNRDB/10.)
      ALPHA=SQRT(2.)*CNR*PT*SIN(PI/PT)/PI
      DSEED=1973245860.D00
C
C  CLEAR SUMP AND SUMY MATRICES.
C  SET FIRST ESTIMATE OF Y TO Y0 AND
C  FIRST VARIANCE MATRIX TO P0
C
      DO 120 I=1,IYDIM
         DO 110 J=1,IYDIM
            DO 100 K=1,KMAX
            SUMP(I,J,K)=0.0
            SUMY(J,K)=0.0
  100       CONTINUE
         P(I,J,1)=P0(I,J)
  110    CONTINUE
      Y(I,1)=Y0(I)
  120 CONTINUE
C
C  AVERAGE OVER "ITER" REALIZATIONS OF THE NOISE
C  PROCESS BY INCREMENTING DSEED ON EACH PASS.
C  NOISE SAMPLES ARE GENERATED BY SUBROUTINE
C  GGNML.
C
      DO 500 I=1,ITER
      CALL GGNML(DSEED,KMPT,N)
C
C  COMPUTE SEQUENCES OF Y AND P FOR ALL K
C
         KMAX=KMAX-1
         DO 400 K=1,KMAX
         KK=IPT*(K-1)
C
C  COMPUTE A-PRIORI UPDATE OF STATE VECTOR
C
            ARGSUP=0.0
            DO 210 IND=1,IYDIM
            ARGSUP=PHI(IYDIM,IND)*Y(IND,K)+ARGSUP
  210       CONTINUE
C
C  SUMS AND SUMC ARE THE CORRELATIONS BETWEEN Z
C  AND THE SINE AND COSINE, RESPECTIVELY, OF THE
C  A-PRIORI ESTIMATE OF THE PHASE.
C
            SUMC=0.0
            SUMS=0.0
            DO 300 J=1,IPT
            N(KK+J)=N(KK+J)/SQRT(CNR*PT)
            CON=2.*PI*FLOAT(J-1)/PT
            ARG=CON+ARGSUP
            Z=(ALPHA/(CNR*PT))*COS(CON+YACT(IYDIM,K))+
```

```
     *       N(KK+J)
             SUMS=Z*SIN(ARG)+SUMS
             SUMC=Z*COS(ARG)+SUMC
  300        CONTINUE
C
C  UPDATE Y AND P USING SIMULATED DATA AND PLANT
C  MODEL.
C
           CALL NEWP(P,PO,PHI,Q,IYDIM,SUMC,ALPHA,K,KMAX,
     *     WKAREA,KWD,N)
           CALL NEWY(Y,PHI,P,IYDIM,SUMS,ALPHA,K,KMAX,PI)
           CALL SUMM(SUMY,SUMP,Y,P,IYDIM,K,KMAX)
  400      CONTINUE
C
C  INCREMENT DSEED.
C
        KMAX=KMAX+1
        DSEED=DSEED+100.D00
  500 CONTINUE
C
C  COMPUTE AVERAGE Y AND P FROM SUMMATION OF ALL
C  "ITER" REALIZATION OF NOISE PROCESS.
C
        DO 620 K=1,KMAX
           DO 610 J=1,IYDIM
              DO 600 I=1,IYDIM
              P(I,J,K)=SUMP(I,J,K)/FLOAT(ITER)
  600         CONTINUE
           Y(J,K)=SUMY(J,K)/FLOAT(ITER)
  610      CONTINUE
  620 CONTINUE
C
C
        RETURN
        END
```

```
      SUBROUTINE NEWP(P,PO,PHI,Q,IYDIM,SUMC,ALPHA,K,KMAX,
     *WKAREA,KWD,S)
      DIMENSION P(IYDIM,IYDIM,KMAX),PHI(IYDIM,IYDIM)
      DIMENSION Q(IYDIM,IYDIM),PO(IYDIM,IYDIM)
      DIMENSION WKAREA(KWD)
C
C  SUBROUTINE NEWP COMPUTES THE NEXT P GIVEN THE
C  LAST P, SUMC, AND THE PLANT MODEL.  SUBROUTINE
C  LINV3F IS USED TO INVERT MATRICES WHEN IYDIM
C  IS NOT EQUAL TO ONE.
C
      DO 400 I=1,IYDIM
         DO 300 J=1,IYDIM
         DUMMYP=0.0
            DO 200 M=1,IYDIM
               DO 100 N=1,IYDIM
               DUMMYP=PHI(I,N)*P(N,M,K)*PHI(J,M)+DUMMYP
  100          CONTINUE
  200       CONTINUE
         PO(I,J)=DUMMYP+Q(I,J)
  300    CONTINUE
  400 CONTINUE
      IF(IYDIM.EQ.1) GOTO 720
      D1=1.
      CALL LINV3F(PO,S,1,IYDIM,IYDIM,D1,D2,WKAREA,IER)
      IF(IER.EQ.130)GOTO 700
  500 PO(IYDIM,IYDIM)=PO(IYDIM,IYDIM)+ALPHA*SUMC
      CALL LINV3F(PO,S,1,IYDIM,IYDIM,D1,D2,WKAREA,IER)
      IF(IER.EQ.130)GOTO 710
  510 DO 610 I=1,IYDIM
          DO 600 J=1,IYDIM
          P(I,J,K+1)=PO(I,J)
  600     CONTINUE
  610 CONTINUE
C
C
      RETURN
  700 PRINT *, "SINGULAR MATRIX ENCOUTERED IN NEWP"
      PRINT *,     "LED BY FIRST OCCURENCE OF LINV3F"
      GOTO 500
C
  710 PRINT *, "SINGULAR MATRIX ENCOUNTERED IN NEWP"
      PRINT *, "CALLED BY SECOND OCCURENCE OF LINV3F"
      GOTO 510
C
  720 P(1,1,K+1)=1./((1./PO(1,1))+ALPHA*SUMC)
C
C
      RETURN
      END
```

```
      SUBROUTINE NEWY(Y,PHI,P,IYDIM,SUMS,ALPHA,K,KMAX,PI)
      DIMENSION Y(IYDIM,KMAX),PHI(IYDIM,IYDIM)
      DIMENSION P(IYDIM,IYDIM,KMAX)
C
C  SUBROUTINE NEWY COMPUTES THE NEXT Y GIVEN THE
C  LAST Y, THE NEW P, SUMS, AND THE PLANT MODEL.  THE
C  PHASE, Y(IYDIM,K+1), IS RETURNED MODULO-2*PI
C
      DO 200 I=1,IYDIM
      DUMMYY=0.0
         DO 100 J=1,IYDIM
         DUMMYY=PHI(I,J)*Y(J,K)+DUMMYY
  100    CONTINUE
      Y(I,K+1)=DUMMYY-P(I,IYDIM,K+1)*ALPHA*SUMS
  200 CONTINUE
      Y(IYDIM,K+1)=AMOD(Y(IYDIM,K+1),PI)
C
C
      RETURN
      END
```

```
      SUBROUTINE SUMM(SUMY,SUMP,Y,P,IYDIM,K,KMAX)
      DIMENSION SUMY(IYDIM,KMAX),SUMP(IYDIM,IYDIM,KMAX)
      DIMENSION Y(IYDIM,KMAX),P(IYDIM,IYDIM,KMAX)
C
C  SUBROUTINE SUMM ACCUMULATES A SUMMATION OF P
C  AND Y FOR ALL "ITER" REALIZATIONS OF THE NOISE
C  PROCESS.
C
  100 DO 300 I=1,IYDIM
         DO 200 J=1,IYDIM
         SUMP(I,J,K)=P(I,J,K)+SUMP(I,J,K)
  200    CONTINUE
      SUMY(I,K)=Y(I,K)+SUMY(I,K)
  300 CONTINUE
      IF(K.LT.KMAX) RETURN
      IF(K.GT.KMAX) GOTO 400
      K=K+1
      GOTO 100
C
  400 K=KMAX
C
C
      RETURN
      END
```

VITA

Martin B. Mark was born on 17 December 1957 in Indianapolis, Indiana. He entered the Purdue University school of engineering at West Lafayette, IN, in the fall of 1975 and graduated from the honors program in the top 10% of his class in May 1979 with a BS degree in Electrical Engineering. Upon graduation, he was granted a commission as a Second Lieutenant in the U.S. Air Force and was disignated a distinguished graduate of AFROTC. His first assignment was to the AFIT at Wright-Patterson AFB, Dayton, OH, where he pursued a MS in Electrical Engineering in the Electro-Optics program. His first assignment after leaving AFIT was to the Air Force Space Division at Los Angeles AFS, Los Angeles, CA, where he went to work for the Deputy for Defense Support.

Permanent Address: 8202 North Illinois St.
Indianapolis, IN 46260

UNCLASSIFIED

SECURITY CLASSIFICATION OF THIS PAGE (When Data Entered)

REPORT DOCUMENTATION PAGE		READ INSTRUCTIONS BEFORE COMPLETING FORM
1. REPORT NUMBER: AFIT/GEO/EE/80D-3	2. GOVT ACCESSION NO.: AD-A100 821	3. RECIPIENT'S CATALOG NUMBER
4. TITLE (and Subtitle): OPTICAL PHASE ESTIMATION FROM INTEGRATED SAMPLES OF THE HETERODYNED WAVEFRONT		5. TYPE OF REPORT & PERIOD COVERED: MS Thesis
		6. PERFORMING ORG. REPORT NUMBER
7. AUTHOR(s): Martin B. Mark, 2dLt, USAF		8. CONTRACT OR GRANT NUMBER(s)
9. PERFORMING ORGANIZATION NAME AND ADDRESS: Air Force Institute of Technology AFIT/EN Wright-Patterson AFB, Ohio 45433		10. PROGRAM ELEMENT, PROJECT, TASK AREA & WORK UNIT NUMBERS
11. CONTROLLING OFFICE NAME AND ADDRESS		12. REPORT DATE: December 1980
		13. NUMBER OF PAGES
14. MONITORING AGENCY NAME & ADDRESS (if different from Controlling Office)		15. SECURITY CLASS. (of this report): UNCLASSIFIED
		15a. DECLASSIFICATION DOWNGRADING SCHEDULE

16. DISTRIBUTION STATEMENT (of this Report)

Approved for public release; distribution unlimited.

17. DISTRIBUTION STATEMENT (of the abstract entered in Block 20, if different from Report)

18. SUPPLEMENTARY NOTES

Approved for public release; IAW AFR 190-17

Frederick C. Lynch

Frederick C. LYNCH, Major, USAF
Director of Public Affairs

16 JUN 1981

19. KEY WORDS (Continue on reverse side if necessary and identify by block number)

Charge Coupled Sensors
Extended Kalman Filtering
Integrating Detectors
Nonlinear Estimation
Phase Estimation
Phase Front Determination

20. ABSTRACT (Continue on reverse side if necessary and identify by block number)

A method for using integrating detectors to estimate the phase of an optical wavefront is investigated. The phase and amplitude are assumed to vary slowly compared to the integration time and the integrated samples are shown to be corrupted by white gaussian noise. A maximum a-posteriori nonlinear Kalman filter is derived and simulated for both constant and random walk phase processes. The performance of the filter is compared to its Cramer-Rao lower

DD FORM 1 JAN 73 1473 EDITION OF 1 NOV 65 IS OBSOLETE

UNCLASSIFIED

SECURITY CLASSIFICATION OF THIS PAGE (When Data Entered)

bound and a first order linearized phase-locked loop (PLL). The filter never performs a great deal better than the PLL, but it can be implemented in a low bandwidth system whereas the PLL assumes a wideband system.

The local oscillator is initially assumed to be stabilized in frequency and amplitude, and later a frequency shift is introduced. The filter manages to acquire and track the phase in a high carrier-to-noise ratio (CNR) environment although it does not estimate the frequency shift well. At 30 db CNR, the phase is estimated within about 0.02 radians, whereas the frequency shift estimation error is on the order of 500 kHz for a frequency shift of 2MHz.

END

DATE
FILMED
7-81

DTIC